On the Multi-Hop Performance of Sender-Receiver Synchronization Mechanisms

Pai-Han Huang, *Electrical Engineering-Systems, University of Southern California*
Maulik Desai, *Electrical and Computer Engineering, The Cooper Union*
Xiaofan Qiu, *Electrical and Computer Engineering, Texas A&M University*
Bhaskar Krishnamachari, *Electrical Engineering-Systems, University of Southern California*

Abstract— **Prior work on sender-receiver-based time synchronization in sensor networks can be categorized into two approaches: two-way packet exchange and one-way packet dissemination. We provide a comprehensive analysis of synchronization errors with these two approaches. We find that one-way dissemination approach provides good relative drift estimation and poor drift estimation while the two-way exchange approach provides accurate drift estimation but imprecise relative drift estimation. In average, using one-way scheme can result in significant cumulative propagation error over multiple hops, and using two-way can lead to high variance of propagation error. We develop and analyze a hybrid one-way dissemination/two-way exchange technique, and verify the performance of our hybrid scheme by experiments. The results suggest that this hybrid approach can provide bounded average error propagation in multi-hop settings and significantly lower variance of propagation error.**

I. Introduction

Many applications in wireless sensor networks have to be accomplished through collaboration between several nodes. Accurately synchronized clocks are important in many aspects, eg TDMA based medium access protocol, sleep scheduling techniques, and object tracking application.

Because every node in a wireless sensor network operates independently, clocks within each node may not be synchronous with one another. Thus, a synchronization mechanism is necessary in such environment. In general, due to the various sources of jitters taking place during synchronization processes, synchronization protocols suffer from error. Typical sources of jitter include send time, access time, propagation time, and receive time. A more detailed explaination can be found in [2].

Due to the uniqueness of wireless sensor network environments, many time synchronization protocols which aim at the wireless sensor network environments have been proposed. In general, the existing works that involve sender-receiver synchronization can be categorized into two types. One can be called *one-way dissemination* and the other is *two-way exchange*. While the former needs a synchronized node to disseminate packets to unsynchronized nodes, the latter achieves synchronization by exchanging packets between synchronizaed and unsynchronized nodes. The Flooding Time Synchronization Protocol (FTSP) [2] is one representative protocol of the one-way packet dissemination scheme. The Timing-sync Protocol for Sensor Networks (TPSN) [3] is a representative of the two-way packet exchange scheme, which requires unsynchronized nodes to exchange packets with synchronized nodes back-and-forth [1]. A more detailed descriptions of TPSN and FTSP can be found in the next section.

Drift and relative drift are two critical parameters while doing time synchronization. Drift refers to the offset of the two clocks, the clocks within the reference node and the node that needs synchronization, at the moment of synchronization. Estimation of the drift thus helps to reset the clocks for re-synchronization. Relative drift refers to change in this offset over some period of time. Estimating the rate of this change can be useful in mitigating further clock drift between synchronization events, especially in a sensor network adopting low duty cycle. We undertake a comparative analysis of the synchronization error of the one-way and two-way schemes. According to our analysis, the one-way packet dissemination does better on estimating relative drift, but suffers from a biased drift estimation that can result in unbounded error propagation over multiple hops in average. While the two-way exchange does better on estimating drift, but the high variance of propagation error over multiple hops may not be acceptable. We propose and analyze a hybrid one-way/two-way mechanism that performs more gracefully under multi-hop conditions. From the results of our trace based simulations, the hybrid scheme not only provides bounded error propagation over multiple hops in average, but also produces low variance of propagation error.

This paper is organized as follows: we first present some existing efforts of providing synchronous clocks for sensor networks in Section II, and analyze the synchronization error for one-way, two-way and the hybrid mechanism for a single sender-receiver pair in Section III. We then investigate the multi-hop synchronization error propagation in Section IV. Details of our time stamps collecting experiments are stated in Section V. The three approaches are compared via trace based

The work described here is supported in part by NSF through grants CNS-0347621, CNS-0627028, CCF-0430061, CNS-0325875, NASA through an AIST grant, and the USC Viterbi School of Engineering's Summer Internship program. Any opinions, findings, and conclusions or recommendations expressed in this material are those of the authors and do not necessarily reflect the views of the NSF, NASA, or USC Viterbi School of Engineering.

[1] A different approach to such sender-receiver schemes is receiver-receiver synchronization, exemplified by the Reference Broadcast Synchronization (RBS) mechanism [4]. We do not analyze receiver-receiver mechanisms in this work.

simulations in Section VI. We conclude with a summary and directions for future work in Section VII.

II. Related Works

In order to provide synchronization tasks, it is necessary to do time stamps exchange between synchronized and unsynchronized nodes. The packets transmitted between sensors for synchronization purpose are called synchronization packets. Depending on the synchronization packets exchange strategies, existing works can be categorized into two major types. One is *one-way dissemination* scheme, and the other one is *two-way exchange* scheme.

In two-way exchange scheme, synchronization packets are sent back and forth between synchronized and unsynchronized nodes. One representative work of this scheme is Timing-sync Protocol for Sensor Networks (TPSN) [3]. TPSN is the first protocol which does time stamping in MAC layer, and this time stamping technique is able to reduce medium access time efficiently. Although some analysis and experiment results are presented in [3], the performance analysis of TPSN under multi-hop networks is lacking.

In one-way dissemination scheme, synchronization packets are only transmitted by synchronized nodes and received by unsynchronized nodes. The Flooding Time Synchronization Protocol (FTSP) [2] is one representative protocol of the one-way packet dissemination scheme. In [2], Maroti et al. propose a sophisticated time stamping technique, which is able to reduce various kinds of jitter terms significantly. Although the authors verify the performance of FTSP mainly by experiments, it is short of theoretical analysis of either FTSP or one-way scheme.

Reference Broadcast Synchronization (RBS) [4] is an exception which does not belong to either one-way or two-way scheme. In RBS, a reference beacon is broadcasted by a reference node. Nodes which receive the broadcasted beacon will record its time of arrival and exchange this information with others. Because synchronization packets are only exchanged among reference beacon receivers, one advantage of RBS is able to get rid of sender side jitter terms [4] [3]. RBS is not included in this study.

Readers are recommended to see [1] for an excellent survey of the state of the art in time synchronization and other existing works which are not mentioned here.

In a multi-hop network, a synchronized node drifts away from its reference clock before it provides clock information to its descendent nodes. Consider the following simple example.

There exist a reference node "*ref*" that is responsible for providing reference clock to the whole network, and there are two nodes, node A and B, which need time synchronization. The topology of this network is shown in fig 1. Due to the transmission constraint, node B can only communicate with node A. Therefore, node B shall not initiate its own synchronization task with node A until node A finishes synchronization with node ref. In fig 2, we plot the synchronization events according to an ideal time axis under this situation. Note that, because of the usage of sleep scheduling, the duration between event II and III may be very long. In addition, clock of

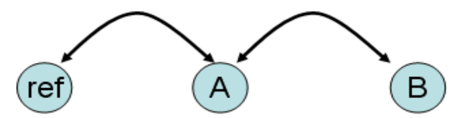

Fig. 1. An example topology for doing synchronization in a multihop network.

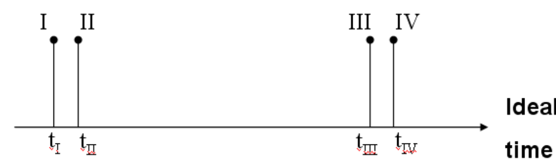

Fig. 2. Synchronization events in ideal time axis.
(I): Beginning of A synchronizing with ref.
(II): End of A synchronizing with ref.
(III): Beginning of B synchronizing with A.
(IV): End of A synchronizing with B.

node A keeps drifting away from node ref's clock due to the imprecision of oscillator it uses. Therefore, before node A is ready to provide clock readings to node B, node A may already posses significant synchronization error corresponding to the reference node. We call this error as "inter-sync error". In practice, skew of oscillator can be as large as $40ppm$, and the duration between event II and III may be as long as 30 minutes. The inter-sync error can be calculated as:

$$\text{inter-sync error} = 2 * 40ppm * 30min = 0.144sec \quad (1)$$

Therefore, node A may posses $144ms$ inter-sync error, compared with the error contributed by synchronization process that is in scale of tens of μs, before it provides its own clock readings to node B. Clearly, inter-sync error can be a dominant term in synchronization error under a multihop, low duty cycle sensor network. However, none of the above works mention it explicitly. In addition, variance of propagation error over multiple hops is another issue which is not fully addressed by existing works. We provide both theoretical analysis and trace based simulations about concerns of variance.

III. Synchronization Error Analysis

We first explain some terminology that will be used in the following contents. By "ideal clock", we are referring to a clock that is capable of measuring time in consistent, and "ideal clock reading" is a clock reading given by an ideal clock. If the nominal frequency of a clock generator i is measured by an ideal clock, than the rate of clock i "drifting away" from its nominal frequency can be computed as $\frac{\text{actual frequency of clock } i}{\text{nominal frequency of clock } i}$. We denote this ratio as B_i. In this paper, we assume that every node has the same nominal frequency. If the clock reading of node i and j at the same instance tk is T_i and T_j, respectively, then, the "drift" between

Ti	A clock reading (time stamp) generated by a node involved in a synchronization process.
ti	The time measured by an ideal clock corresponding to the clock reading Ti.
$D_{ti}^{k\to l}$	The difference of clock readings of node k and l at ti. We call it *drift* at time ti in the following contents.
$RD_{ti\to tj}^{k\to l}$	$RD_{ti\to tj}^{k\to l} = D_{ti}^{k\to l} - D_{tj}^{k\to l}$. We call it *relative drift* from ti to tj in the following contents.
Γ_i	Total transmission and reception delay corresponding to packet i as measured by an ideal clock.
Ti^{ori}	A time stamp has not been calibrated.
Ti^{ideal}	A time stamp that is ideally calibrated.
Ti^{est}	A time stamp that is calibrated by estimation of a synchronization scheme.
$\alpha_{ti\to tj}^{k\to l}$	The estimation of relative drift between node k and l from ti to tj.
$\beta_{ti}^{j\to k}$	The estimation of drift between node j and k at ti.
Θ_{ti}^{j}	Propagation error up to level j at ti.
$\Phi_{ti\to tj}^{k\to l}$	Error of relative drift estimation $\alpha_{ti\to tj}^{k\to l}$.
X_i	Actual frequency of node i's clock generater.
B_i	Ratio of actual and nominal frequency of node i's clock generater.

TABLE I

NOTATIONS

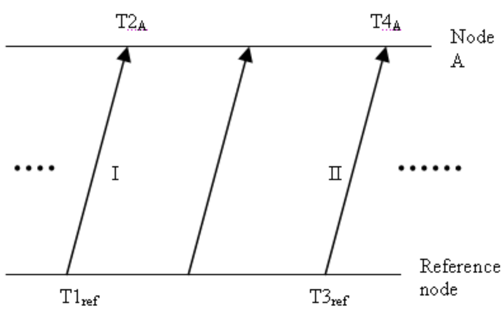

Fig. 3. Message timelines for one-way synchronization scheme

node i and j at tk is $D_{tk}^{i\to j} = T_j - T_i$. Similarly, the drift between i and j at tl can be denoted as $D_{tl}^{i\to j}$. Because of the difference between B_i and B_j, we define the "relative drift" between node i and j from tk to tl as $RD_{tk\to tl}^{i\to j} = D_{tk}^{i\to j} - D_{tl}^{i\to j}$.

According to [2], the possible sources of delays in packet transmission include application layer send-receive times, access time, link layer transmission and reception time, propagation time, interrupt handling time, encoding and decoding time, and byte alignment time. In the following we represent by Γ_i the total delay taken for packet i to be transmitted from one node to another, even after some of the component delay sources are mitigated through sophisticated time stamping techniques such as those proposed in [2].

We first present an analysis of the drift and relative drift for the different schemes for the simplest two-node one-hop setting, and the symbols used in the following contents are listed in Table I.

A. Analysis of One-way Scheme

An example scenario of doing synchronization by using one-way scheme is plotted in Figure 3. The arrows in the figure represent directions of transmitted packets for synchronization purposes. Without loss of generality, we arbitrarily choose two packets, which are denoted by I and II in this figure, for analysis purpose. For clarification, we denote each time stamp Ti with a subscript ref or A to represent the node which generates it. The time relations of packet I and II can be written as follows.

$$\begin{aligned} T2_A &= T1_{ref} + D_{t1}^{ref\to A} + \Gamma_I B_A \\ &\approx T1_{ref} + D_{t1}^{ref\to A} + \Gamma_I \end{aligned} \tag{2}$$

$$\begin{aligned} T4_A &= T3_{ref} + D_{t3}^{ref\to A} + \Gamma_{II} B_A \\ &\approx T3_{ref} + D_{t3}^{ref\to A} + \Gamma_{II} \end{aligned} \tag{3}$$

The B_A term is the ratio of actual frequency and the nominal frequency of clock generator used by node A. The effectiveness of the approximation used in the above equations can be found in Appendix I. Because $D_{t1}^{ref\to A} - D_{t3}^{ref\to A} = RD_{t1\to t3}^{ref\to A}$, subtracting equation (3) from (2), we have,

$$\begin{aligned} RD_{t1\to t3}^{ref\to A} &\approx RD_{t2\to t4}^{ref\to A} \\ = (T2_A - T4_A) &- (T1_{ref} - T3_{ref}) - (\Gamma_I - \Gamma_{II}) \end{aligned} \tag{4}$$

Also, from equation (3), we can get,

$$D_{t3}^{ref\to A} \approx D_{t4}^{ref\to A} = (T4_A - T3_{ref}) - \Gamma_{II} \tag{5}$$

Because the best drift estimation one-way can achieve under this two synchronization packets scenario is $T4_A - T3_{ref}$, using one-way scheme consistently over-estimates the drift by Γ_{II}. Note that, people may use linear regression on multiple synchronization packets to estimate the drift in practice. Since we choose the packet I and II arbitrarily within many synchronization packets in Figure 3, no matter which two packets we choose, the drift estimation using one-way scheme is always larger than actual drift by amount of Γ_{II}. Therefore, we can conclude that using one-way scheme always over-estimates the drift.

On the other hand, we notice that the one-way scheme is capable of providing accurate relative drift estimation. In equation (4), we see the relative drift estimation is influenced by jitters in amount of $\Gamma_I - \Gamma_{II}$. If the nodes involved in this synchronization process are using the identical hardware and software settings, we can expect the mean value of Γ_I

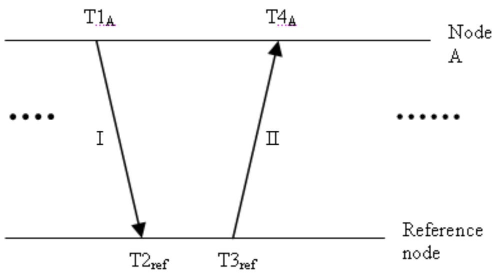

Fig. 4. Message timelines for two-way synchronization schemes

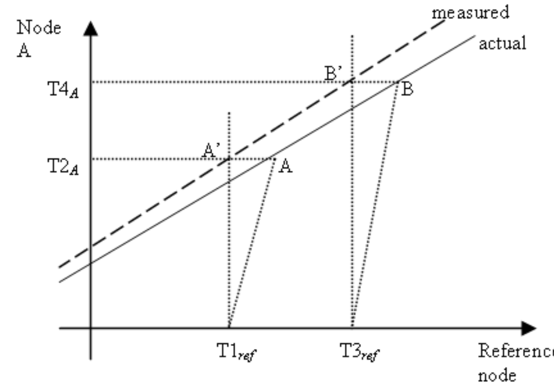

(a)

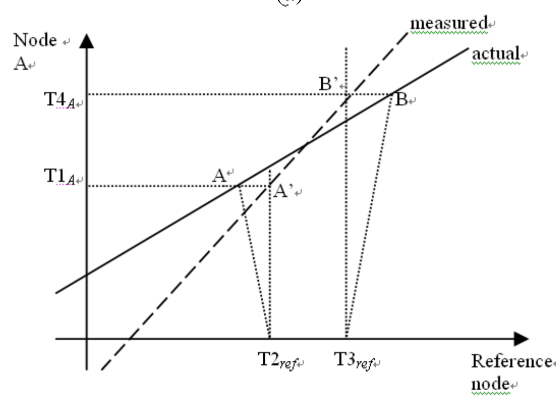

(b)

Fig. 5. Illustration of synchronization errors with (a) one-way and (b) two-way schemes.

and Γ_{II} are approximately the same. Therefore, the relative drift estimation calculated by one-way scheme is precise in average.

B. Analysis of Two-way Scheme

In Figure 4, an example scenario of doing synchronization by using two-way scheme is plotted. The time relations of packet I and II can be written as follows.

$$T2_{ref} = T1_A - D_{t1}^{ref \to A} + \Gamma_I \tag{6}$$

Note that $D_{t3}^{ref \to A} \approx D_{t4}^{ref \to A}$; hence,

$$T4_A = T3_{ref} + D_{t4}^{ref \to A} + \Gamma_{II} \tag{7}$$

Because $D_{t1}^{ref \to A} - D_{t4}^{ref \to A} = RD_{t1 \to t4}^{ref \to A}$, adding equation (6) and (7), we have,

$$\begin{aligned} RD_{t1 \to t4}^{ref \to A} = {} & (T1_A - T2_{ref}) + (T3_{ref} - T4_A) \\ & + (\Gamma_{II} + \Gamma_I) \end{aligned} \tag{8}$$

Subtracting (6) from (7) and using $D_{t1}^{ref \to A} - D_{t4}^{ref \to A} = RD_{t1 \to t4}^{ref \to A}$,

$$\begin{aligned} D_{t4}^{ref \to A} &= \frac{1}{2}[(T1_A - T2_{ref}) - (T3_{ref} - T4_A) \\ &- RD_{t1 \to t4}^{ref \to A} + (\Gamma_I - \Gamma_{II})] \end{aligned} \tag{9}$$

According to [3], the drift estimation can be calculated as,

$$\begin{aligned} & \textit{drift estimation} \\ = {} & \frac{1}{2}[(T1_A - T2_{ref}) - (T3_{ref} - T4_A)] \end{aligned} \tag{10}$$

Therefore, the error of drift estimation by using two-way scheme is,

$$\begin{aligned} & \textit{error of drift estimation} \\ = {} & \frac{1}{2}[RD_{t1 \to t4}^{ref \to A} - (\Gamma_I - \Gamma_{II})] \end{aligned} \tag{11}$$

From equation (8) we notice that, the relative drift estimation is influenced by jitters in amount of $\Gamma_I + \Gamma_{II}$. Because both the Γ_I and Γ_{II} are positive, one potential problem of using two-way scheme is inaccurate relative drift estimation. In addition, by equation (11), the drift estimation precision is also influenced by the duration of a synchronization period length. The longer the period length is, the lower the precision of drift estimation of two-way scheme will be. However, from the same equation we also notice that, if the synchronization process can be done in a short period of time, then the error of two-way drift estimation can be approximated by the difference between two jitter terms.

In [3], the authors do not explicitly propose the method of relative drift estimation. In order to perform a fair comparison between different synchronization schemes, we use a similar way as stated in [3] to find out the corresponding relative drift estimation under two-way scheme as above.

C. A Hybrid Scheme and its analysis

The synchronization errors observed with both one-way and two-way are illustrated in Figure 5 (a) and (b). In these figures, the X-axis and Y-axis represents clock reading of reference node and node A, respectively. The solid line represents the real relation of clock readings of reference node and node A. The measured relation is plotted as dotted lines. If Γ_I and Γ_{II} has the same distribution, then the one-way scheme produces precise relative drift estimation but over-estimates drift in average. Again, if Γ_I and Γ_{II} have the same distribution, then we can conclude that the two-way scheme over-estimates relative drift.

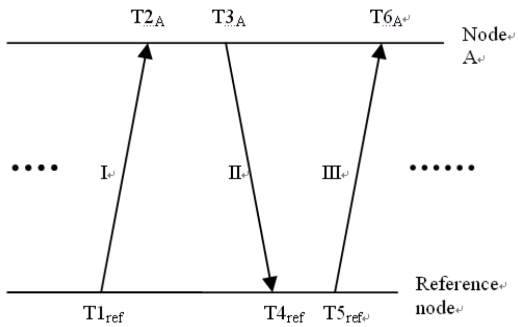

Fig. 6. Message timelines for hybrid synchronization schemes

We propose a hybrid scheme that attempts to combine the best features of the one-way and two-way schemes to give better precision. The basic idea is to obtain a relative drift estimation expression similar to one-way but use it in the drift estimation for two-way. An example of synchronization packet exchange scenario by using hybrid scheme is shown in Figure 6. The time relations of packet I, II, and III of this figure can be written as follows.

$$T2_A = T1_{ref} + D_{t1}^{ref\to A} + \Gamma_I \quad (12)$$

$$T4_{ref} = T3_A - D_{t3}^{ref\to A} + \Gamma_{II} \quad (13)$$

$$T6_A = T5_{ref} + D_{t5}^{ref\to A} + \Gamma_{III} \quad (14)$$

Because $D_{t5}^{ref\to A} \approx D_{t6}^{ref\to A}$, subtracting equation (14) from (13) and substituting $RD_{t3\to t6}^{ref\to A} = D_{t3}^{ref\to A} - D_{t6}^{ref\to A}$, we get,

$$\begin{aligned} &2D_{t6}^{ref\to A} + RD_{t3\to t6}^{ref\to A} = \\ &(T6_A - T4_{ref}) - (T5_{ref} - T3_A) - (\Gamma_{III} - \Gamma_{II}) \end{aligned} \quad (15)$$

Since $D_{t1}^{ref\to A} - D_{t5}^{ref\to A} = RD_{t1\to t5}^{ref\to A}$, after subtracting equation (14) from (12), we have,

$$\begin{aligned} &RD_{t1\to t5}^{ref\to A} = \\ &(T2_A - T6_A) - (T1_{ref} - T5_{ref}) - (\Gamma_I - \Gamma_{III}) \end{aligned} \quad (16)$$

Because $RD_{t1\to t5}^{ref\to A} \approx RD_{t2\to t6}^{ref\to A}$, and $RD_{t3\to t6}^{ref\to A} = RD_{t2\to t6}^{ref\to A} \frac{T6_A - T3_A}{T6_A - T2_A}$, from equation (16) we can have,

$$\begin{aligned} RD_{t3\to t6}^{ref\to A} &= \frac{T6_A - T3_A}{T6_A - T2_A}[(T5_{ref} - T1_{ref}) \\ &- (T6_A - T2_A) + (\Gamma_{III} - \Gamma_I)] \end{aligned} \quad (17)$$

Replace the relative drift term in equation (15) with equation (17) we get,

$$\begin{aligned} D_{t6}^{ref\to A} &= \frac{1}{2}[(T6_A - T4_{ref}) - (T5_{ref} - T3_A) \\ &+ \frac{T6_A - T3_A}{T6_A - T2_A}[(T6_A - T2_A) - (T5_{ref} - T1_{ref}) \\ &- (\Gamma_{III} - \Gamma_I)] - (\Gamma_{III} - \Gamma_{II})] \end{aligned} \quad (18)$$

From equations (17) and (18), if Γ_I, Γ_{II}, and Γ_{III} have the same distribution, then using hybrid scheme provides not only precise relative drift estimation, but also accurate drift estimation in average (Because $E[\Gamma_i] = constant \forall i \in I, II, III$, all Γ terms are cancelled out.). We will further evaluate the multihop performance of this hybrid scheme in the next section.

A brief summary of the above analyses can be found in Table II.

IV. Analysis of Synchronization Error under Multihop Situations

Because of the existence of inter-sync error, a synchronized node, say node A, may already possess significant error before another node tries to synchronize with it. If node A uses relative drift estimation to calibrate its clock before providing readings to other nodes, the inaccuracy of relative drift estimation still deteriorates the synchronization precision. The longer the inter-synchronization period is, the larger the propagation error will be. Obviously, the inter-sync error is not a negligible error source when inter synchronization period is long. In multihop networks with sleep-scheduling which can increase the inter-synchronization intervals, inter-sync error may be more severe.

Because we are able to estimate relative drift under different synchronization schemes, we have options of compensating inter-sync error by using relative drift estimation or not. We analyze both cases separately in the following sections. The symbols used in the following analysis are listed in Table I. Note that, for simplicity, we make the following assumptions:

1) The inter synchronization period length is the same for every synchronization instance and every scheme, and is denoted by T_{inter}. For example, the duration between time stamps $T4$ and $T5$ in Figure 7 is T_{inter}.
2) The length of the duration between two consecutive time stamps of the same node within one synchronization process is a constant for every synchronization instance and every scheme, and its value is denoted as T_{intra}. For example, the duration between time stamps $T2$ and $T4$ in Figure 7 is T_{intra}.
3) Every node is equipped with identical hardware and software, and the distance between each pair of nodes is approximately the same. Consequently, all jitter terms, ie Γ, have the same distribution.
4) Every synchronization instance is independent with each other.
5) Every clock generator's actual frequency remains constant, and is independent with each other.

For brevity, we only present the main conclusions under different scenarios in this section, and the detail derivations can be found in Appendix III.

A. Propagation error without relative drift compensation

1) One-way scheme: Consider a synchronization scenario as plotted in Figure 7. From Appendix III-A, the propagation error Θ_{t4}^{i+1} and Θ_{t8}^{i+2} thus becomes,

one-way drift estimation	$\beta_{t4}^{ref\to A} = T4_A - T3_{ref}$
error of one-way drift estimation	$-\Gamma_{II}$
one-way relative drift estimation	$\alpha_{t1\to t3}^{ref\to A} = (T2_A - T4_A) - (T1_{ref} - T3_{ref})$
error of one-way relative drift estimation	$-(\Gamma_I - \Gamma_{II})$
two-way drift estimation	$\beta_{t4}^{ref\to A} = \frac{1}{2}[(T1_A - T2_{ref}) - (T3_{ref} - T4_A)$
error of two-way drift estimation	$\frac{1}{2}[-RD_{t1\to t4}^{ref\to A} + (\Gamma_I - \Gamma_{II})]$
two-way relative drift estimation	$\alpha_{t1\to t4}^{ref\to A} = (T1_A - T2_{ref}) + (T3_{ref} - T4_A)$
error of two-way relative drift estimation	$(\Gamma_{II} + \Gamma_I)$
hybrid drift estimation	$\beta_{t6}^{ref\to A} = \frac{1}{2}[(T6_A - T4_{ref}) - (T5_{ref} - T3_A) + \frac{T6_A - T3_A}{T6_A - T2_A}[(T6_A - T2_A) - (T5_{ref} - T1_{ref})]]$
error of hybrid drift estimation	$\frac{1}{2}[-\frac{T6_A - T3_A}{T6_A - T2_A}(\Gamma_{III} - \Gamma_I) - (\Gamma_{III} - \Gamma_{II})]$
hybrid relative drift estimation	$\alpha_{t1\to t5}^{ref\to A} = (T2_A - T6_A) - (T1_{ref} - T5_{ref})$
error of hybrid relative drift estimation	$-(\Gamma_I - \Gamma_{III})$

TABLE II
CONCLUSIONS OF PAIR-WISE ANALYSIS

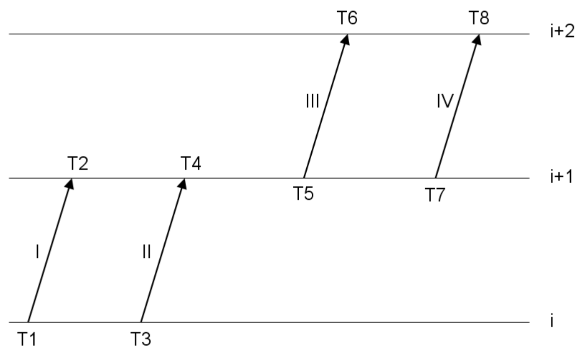

Fig. 7. An example scenario for doing synchronization in a multihop network using one-way scheme.

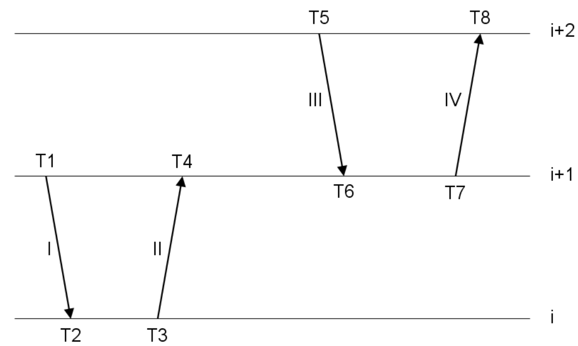

Fig. 8. An example scenario for doing synchronization in a multihop network using two-way scheme.

$$
\begin{aligned}
\Theta_{t4}^{i+1} &= T4^{ideal} - T4^{est} \\
&= (T4^{ori} - D_{t4}^{i\to i+1}) - (T4^{ori} - \beta_{t4}^{i\to i+1}) \\
&= -D_{t4}^{i\to i+1} + \beta_{t4}^{i\to i+1} \\
&= T3^{ideal} - T3^{est} + \Gamma_{II} \qquad (19)
\end{aligned}
$$

$$
\Theta_{t8}^{i+2} = \Theta_{t4}^{i+1} + RD_{t4\to t8}^{i\to i+1} + \Gamma_{IV} \qquad (20)
$$

From equation (20), the propagation error up to $i+2$ hop is composed of the error generated in prior hop Θ_{t4}^{i+1}, relative drift $RD_{t4\to t8}^{i\to i+1}$, and a jitter term Γ_{IV}. From equation (19), if the reference node is located in level i, then $T3^{ideal} = T3^{est}$. Therefore, the propagation error up to $i+1$ hop is merely the jitter term. In addition, as shown in Appendix II, the expected value of $RD_{t4\to t8}^{i\to i+1}$ is zero if T_{inter} and T_{intra} are constants for every synchronization iterations. Therefore, the expected value of propagation error of one-way scheme without inter-sync error compensation will be linearly increasing with respect to hop count distance.

2) Two-way scheme: Consider a synchronization scenario as plotted in Figure 8. From Appendix III-B, the propagation error can be computed as,

$$
\begin{aligned}
\Theta_{t4}^{i+1} &= T4^{ideal} - T4^{est} = -D_{t4}^{i\to i+1} + \beta_{t4}^{i\to i+1} \\
&= \frac{1}{2}[(T2^{ideal} - T2^{est}) + (T3^{ideal} - T3^{est}) \\
&+ RD_{t1\to t4}^{i\to i+1} - (\Gamma_I - \Gamma_{II})] \qquad (21)
\end{aligned}
$$

$$
\begin{aligned}
\Theta_{t8}^{i+2} &= \frac{1}{2}[-2(D_{t4}^{i\to i+1} - \beta_{t4}^{i\to i+1}) + RD_{t4\to t6}^{i\to i+1} \\
&+ RD_{t4\to t7}^{i\to i+1} + RD_{t5\to t8}^{i+1\to i+2} - (\Gamma_{III} - \Gamma_{IV})] \\
&= \frac{1}{2}[2\Theta_{t4}^{i+1} + RD_{t4\to t6}^{i\to i+1} + RD_{t4\to t7}^{i\to i+1} \\
&+ RD_{t5\to t8}^{i+1\to i+2} - (\Gamma_{III} - \Gamma_{IV})] \qquad (22)
\end{aligned}
$$

From equation (22), the propagation error in prior hop will be carried to the next hop. According to Appendix II and the assumption 2), the mean value of $RD_{t1\to t4}^{i\to i+1}$ in equation (21) will be zero. Thus, by the assumption 3), the mean value of Θ_{t4}^{i+1} will also be zero if the reference node is located in level i. In other words, the expected value of error that will be propagated to further hops is zero. Consequently, the expected value of propagation error up to $i+2$ is also zero. However, one potential problem of using two-way without inter-sync compensation is the high variance of propagation error. As we can see from equation (22), two-way scheme is highly influenced by relative drift terms, and the impact of variance caused by relative drift terms can be found in Appendix IV.

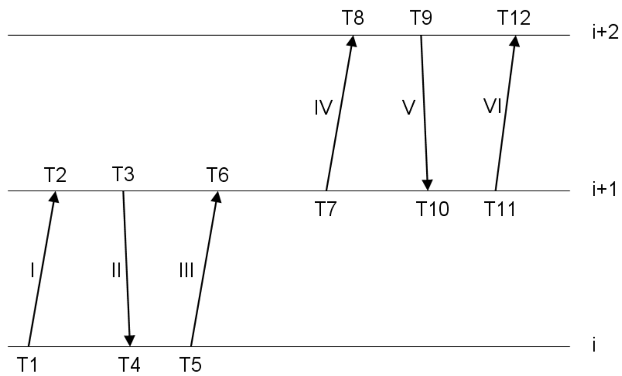

Fig. 9. An example scenario for doing synchronization in a multihop network using hybrid scheme.

Although the mean value of propagation error is zero, but we may end up with huge propagation error in some instances.

3) Hybrid scheme: Consider a synchronization scenario as plotted in Figure 9. From Appendix III-C, the propagation error can be computed as,

$$\begin{aligned}\Theta_{t6}^{i+1} &= T6^{ideal} - T6^{est} = -D_{t6}^{i\to i+1} + \beta_{t6}^{i\to i+1} \\ &\approx \frac{1}{2}[(T4^{ideal} - T4^{est}) + (T5^{ideal} - T5^{est}) \\ &+ \frac{T_{intra}}{2T_{intra}}[(T5^{ideal} - T5^{est}) \\ &- (T1^{ideal} - T1^{est}) + (\Gamma_{III} - \Gamma_I)] \\ &+ (\Gamma_{III} - \Gamma_{II})] \end{aligned} \tag{23}$$

$$\begin{aligned}\Theta_{t12}^{i+2} &= T12^{ideal} - T12^{est} \\ &= -D_{t12}^{i+1\to i+2} + \beta_{t12}^{i+1\to i+2} \\ &\approx \frac{1}{2}[(T10^{ideal} - T10^{est}) + (T11^{ideal} - T11^{est}) \\ &+ \frac{T_{intra}}{2T_{intra}}[(T11^{ideal} - T11^{est}) \\ &- (T7^{ideal} - T7^{est}) + (\Gamma_{VI} - \Gamma_{IV})] + (\Gamma_{VI} - \Gamma_V)] \\ &\approx \frac{1}{2}[2\Theta_{t6}^{i+1} + (RD_{t6\to t10}^{i\to i+1} + \frac{3}{2}RD_{t6\to t11}^{i\to i+1}) \\ &- \frac{1}{2}RD_{t6\to t7}^{i\to i+1} + (\frac{3}{2}\Gamma_{VI} - \frac{1}{2}\Gamma_{IV} - \Gamma_V)] \end{aligned} \tag{24}$$

For the same reason as prior analysis, if the reference node is located in level i, we can expect the average propagation error up to $i+1$ hop will be zero by observing equation (23). In addition, we can also conclude the expected propagation error up to $i+2$ is also zero from equation (24). However, it is also noticeable that using hybrid scheme without inter-sync error compensation may also lead to high variance of propagation error because of several relative drift terms in equation (24).

B. Propagation error with relative drift compensation

1) One-way scheme: Consider the scenario plotted in Figure 7. From Appendix III-D, the propagation error and error of relative drift estimation can be calculated as,

$$\begin{aligned}\Theta_{t4}^{i+1} &= T4^{ideal} - T4^{est} \\ &= (T4^{ori} - D_{t4}^{i\to i+1}) - (T4^{ori} - \beta_{t4}^{i\to i+1}) \\ &= -D_{t4}^{i\to i+1} + \beta_{t4}^{i\to i+1} \\ &= T3^{ideal} - T3^{est} + \Gamma_{II} \end{aligned} \tag{25}$$

$$\begin{aligned}\Phi_{t2\to t4}^{i\to i+1} &= RD_{t2\to t4}^{i\to i+1} - \alpha_{t2\to t4}^{i\to i+1} \\ &= (T3^{ideal} - T3^{est}) - (T1^{ideal} - T1^{est}) - (\Gamma_I - \Gamma_{II}) \end{aligned} \tag{26}$$

$$\begin{aligned}\Theta_{t8}^{i+2} &= T8^{ideal} - T8^{est} \\ &= T7^{ideal} - T7^{est} + \Gamma_{IV} \\ &\approx (T3^{ideal} - T3^{est}) + \Gamma_{II} \\ &+ \frac{T_{inter} + T_{intra}}{T_{intra}}[(T3^{ideal} - T3^{est}) \\ &- (T1^{ideal} - T1^{est}) - (\Gamma_I - \Gamma_{II})] \\ &= \Theta_{t4}^{i+1} + \frac{T_{inter} + T_{intra}}{T_{intra}}\Phi_{t2\to t4}^{i\to i+1} + \Gamma_{IV} \end{aligned} \tag{27}$$

$$\begin{aligned}\Phi_{t6\to t8}^{i+1\to i+2} &= RD_{t6\to t8}^{i+1\to i+2} - \alpha_{t6\to t8}^{i+1\to i+2} \\ &= \Phi_{t2\to t4}^{i\to i+1} - (\Gamma_{III} - \Gamma_{IV}) \end{aligned} \tag{28}$$

If the reference node is located in level i, then the mean propagation error up to $i+1$ hop becomes $E[\Gamma]$ by taking expectation on equation (25). Taking expectation on equation (26), the mean of $\Phi_{t2\to t4}^{i\to i+1}$ becomes zero. Consequently, from equation (27), the expected propagation error up to $i+2$ hop is $2E[\Gamma]$. By induction, using one-way with inter-sync error compensation will lead to linearly increasing average propagation error.

2) Two-way scheme: Refer to an example scenario plotted in Figure 8. From Appendix III-E, the propagation error and error of relative drift estimation can be calculated as,

$$\begin{aligned}\Theta_{t4}^{i+1} &= T4^{ideal} - T4^{est} = -D_{t4}^{i\to i+1} + \beta_{t4}^{i\to i+1} \\ &= \frac{1}{2}[(T2^{ideal} - T2^{est}) + (T3^{ideal} - T3^{est}) \\ &+ RD_{t1\to t4}^{i\to i+1} - (\Gamma_I - \Gamma_{II})] \end{aligned} \tag{29}$$

$$\begin{aligned}\Phi_{t1\to t4}^{i\to i+1} &= RD_{t1\to t4}^{i\to i+1} - \alpha_{t1\to t4}^{i\to i+1} \\ &= (T2^{est} - T2^{ideal}) + (T3^{est} - T3^{ideal}) \\ &+ (\Gamma_I + \Gamma_{II}) \end{aligned} \tag{30}$$

$$\begin{aligned}\Theta_{t8}^{i+2} &= -D_{t8}^{i+1\to i+2} - \beta_{t8}^{i+1\to i+2} \\ &= \frac{1}{2}[(T6^{ideal} - T6^{est}) + (T7^{ideal} - T7^{est}) \\ &+ RD_{t5\to t8}^{i+1\to i+2} - (\Gamma_{III} - \Gamma_{IV})] \\ &\approx \Theta_{t4}^{i+1} - \frac{2T_{inter} + T_{intra}}{2T_{intra}}\Phi_{t1\to t4}^{i\to i+1} \\ &+ \frac{1}{2}RD_{t5\to t8}^{i+1\to i+2} + \frac{1}{2}(\Gamma_{IV} - \Gamma_{III}) \end{aligned} \tag{31}$$

$$
\begin{aligned}
\Phi_{t5\to t8}^{i+1\to i+2} &= RD_{t5\to t8}^{i+1\to i+2} - \alpha_{t5\to t8}^{i+1\to i+2} \\
&= (T7^{ideal} - T7^{est}) - (T6^{ideal} - T6^{est}) \\
&+ (\Gamma_{III} + \Gamma_{IV}) \\
&= \Phi_{t1\to t4}^{i\to i+1} + (\Gamma_{III} + \Gamma_{IV})
\end{aligned} \tag{32}
$$

By observing the above equations we have two findings. First, drift estimation error in current hop will be carried to the next hop. Second, the relative drift estimation keeps adding error in every hop and also deteriorates the drift estimation in next hop. Therefore, multihop propagation error will keep accumulate quadratically.

3) Hybrid scheme: Consider the synchronization scenario as plotted in Figure 9. From Appendix III-F, the propagation error and error of relative drift estimation can be computed as,

$$
\begin{aligned}
\Theta_{t6}^{i+1} &= T6^{ideal} - T6^{est} = -D_{t6}^{i\to i+1} + \beta_{t6}^{i\to i+1} \\
&\approx \frac{1}{2}[(T4^{ideal} - T4^{est}) + (T5^{ideal} - T5^{est}) \\
&+ \frac{T_{intra}}{2T_{intra}}[(T5^{ideal} - T5^{est}) \\
&- (T1^{ideal} - T1^{est}) + (\Gamma_{III} - \Gamma_{I})] \\
&+ (\Gamma_{III} - \Gamma_{II})]
\end{aligned} \tag{33}
$$

$$
\begin{aligned}
\Phi_{t3\to t6}^{i\to i+1} &= RD_{t3\to t6}^{i\to i+1} - \alpha_{t3\to t6}^{i\to i+1} \\
&= \frac{T_{intra}}{2T_{intra}}[(T5^{ideal} - T5^{est}) \\
&- (T1^{ideal} - T1^{est}) + (\Gamma_{III} - \Gamma_{I})]
\end{aligned} \tag{34}
$$

$$
\begin{aligned}
\Theta_{t12}^{i+2} &= -D_{t12}^{i+1\to i+2} + \beta_{t12}^{i+1\to i+2} \\
&= \frac{1}{2}[(T10^{ideal} - T10^{est}) \\
&+ (T11^{ideal} - T11^{est})(1 + \frac{T12^{ori} - T9^{ori}}{T12^{ori} - T8^{ori}}) \\
&- (T7^{ideal} - T7^{est})\frac{T12^{ori} - T9^{ori}}{T12^{ori} - T8^{ori}} \\
&+ (\frac{T12^{ori} - T9^{ori}}{T12^{ori} - T8^{ori}}(\Gamma_{VI} - \Gamma_{IV}) + \Gamma_{VI} - \Gamma_{V})] \\
&\approx \frac{1}{2}[2\Theta_{t6}^{i+1} + 3\Phi_{t3\to t6}^{i\to i+1} \\
&+ (\frac{T_{intra}}{2T_{intra}}(\Gamma_{VI} - \Gamma_{IV}) + \Gamma_{VI} - \Gamma_{V})]
\end{aligned} \tag{35}
$$

$$
\begin{aligned}
\Phi_{t9\to t12}^{i+1\to i+2} &= RD_{t9\to t12}^{i+1\to i+2} - \alpha_{t9\to t12}^{i+1\to i+2} \\
&= \frac{T_{intra}}{2T_{intra}}[(T11^{ideal} - T11^{est}) \\
&- (T7^{ideal} - T7^{est}) + (\Gamma_{VI} - \Gamma_{IV})] \\
&= \frac{1}{2}[(\Gamma_{VI} - \Gamma_{IV}) + 2\Theta_{t3\to t6}^{i\to i+1}]
\end{aligned} \tag{36}
$$

If the reference node is located in level i, from equation (24), the expected value of $\Phi_{t3\to t6}^{i\to i+1}$ is zero. In addition, the mean of $\Theta_{t6}^{i\to i+1}$ is also zero. Thus, propagation error generated in one hop will not be carried to next hop in average. The expected value of propagation error up to $i+2$ hop is zero again.

V. Experiments

A. Experiment Setup

In order to verify the performance of the hybrid scheme, we collect time stamps on wireless sensors and simulate three different synchronization schemes (One-way, Two-way, and Hybrid) offline using simulation tools. Comprehensive data analysis was done by calculating and comparing the synchronization errors over multiple hops across different schemes.

Detailed descriptions of experimental environment are given as follows,

- We use 20 Tmote and mark each of them with a unique physical ID number, from 1 to 20. Every mote is within the transmission range of others. Therefore, every mote is capable of communicating directly with any other mote in our experiment.
- Each synchronization packet includes the following information: Round Number, Sender ID, Receiver ID, Sender Time Stamp, and Receiver Time Stamp, which are explained as follows:
    1) Sender ID and Receiver ID: They are the same as the Physical ID assigned to each node.
    2) Round Number: A round is consisted of a sequential synchronization packets sent through Node ID 1 to Node ID 20. Each Round number consists of 20 sending cycles. Explained in more details in data collection section.
    3) Time Stamp: The clock reading when a sender node transmits a synchronization packet. The difference between Sender Time Stamp and Receiver Time Stamp is the drift estimation between two nodes. However, there are error in time stamps. A detailed error analysis in time stamp is available in [3]. In our experiments, we do time stamping in application layer. In other words, we record the clock reading when a synchronization packet is sent by application layer, and the reading when application layer is notified of the arrival of a synchronization packet. Therefore, a non-negligible time delay between the recorded time and actual time is expected [3]. According to [3] and [2], this delay could be significantly decreased by using MAC layer time stamp and other sophisticated techniques. Application layer time stamp will result an error of millisecond, while MAC layer time stamp is capable of achieving an error of microsecond level. The purpose of this experiment is to compare three different schemes. Therefore, as long as time stamp technique is consistent, the result should reveal the same conclusion using either time stamp technique.

Our data collection experiment proceeds as follows:

1) At time T=0, the node with physical ID 1 starts to broadcast ten synchronization packets to the rest of

One-way w/o inter-sync error compensation	$\Theta_{t8}^{i+2} = \Theta_{t4}^{i+1} + RD_{t4\to t8}^{i\to i+1} + \Gamma_{IV}$
One-way w/ inter-sync error compensation	$\Theta_{t8}^{i+2} \approx \Theta_{t4}^{i+1} + \frac{T_{inter}+T_{intra}}{T_{intra}}\Phi_{t2\to t4}^{i\to i+1}$
Two-way w/o inter-sync error compensation	$\frac{1}{2}[2\Theta_{t4}^{i+1} + RD_{t4\to t6}^{i\to i+1} + RD_{t4\to t7}^{i\to i+1} + RD_{t5\to t8}^{i+1\to i+2} - (\Gamma_{III} - \Gamma_{IV})]$
Two-way w/ inter-sync error compensation	$\Theta_{t8}^{i+2} \approx \Theta_{t4}^{i+1} - \frac{3}{2}\Phi_{t1\to t4}^{i\to i+1}$
Hybrid w/o inter-sync error compensation	$\frac{1}{2}[2\Theta_{t6}^{i+1} + RD_{t6\to t10}^{i\to i+1} + \frac{3}{2}RD_{t6\to t11}^{i\to i+1} - \frac{1}{2}RD_{t6\to t7}^{i\to i+1} + (\frac{3}{2}\Gamma_{VI} - \frac{1}{2}\Gamma_{IV} - \Gamma_{V})]$
Hybrid w/ inter-sync error compensation	$\Theta_{t12}^{i+2} \approx \frac{1}{2}[2\Theta_{t6}^{i+1} + 3\Phi_{t3\to t6}^{i\to i+1} + (\frac{1}{2}\Gamma_{VI} - \Gamma_{IV} + \Gamma_{VI} - \Gamma_{V})]$

TABLE III

SUMMARY OF MULTIHOP ANALYSIS CONCLUSIONS UNDER DIFFERENT SYNCHRONIZATION SCHEMES. ALL PROPAGATION ERRORS ARE PRESENTED IN ITERATIVE FORM.

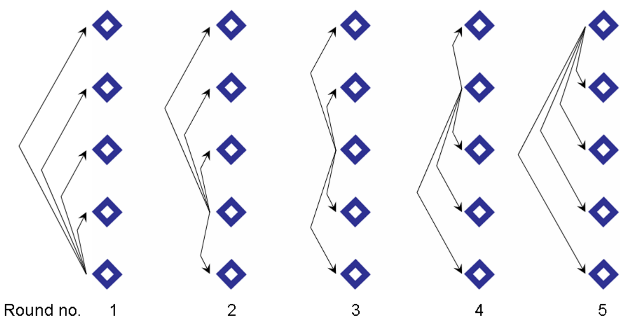

Fig. 10. An illustration of sending round for a 5-node network.

nodes at an interval of 10 ms. The transmission of ten packets at each node consists one sending cycle.

If a node receives a synchronization packet, it will record the sending time stamp, sender ID, and the corresponding local receive time stamp for that packet.

2) Nodes in the network transmit packets in sequence of their physical ID. The node with physical ID $i+1$ will start its sending cycle after 150 *ms* of the first received packet from node i to avoid overlapping with previous node packet transmission. Each receiver will only accept the first uncorrupted synchronization packet it receives, discarding the following redundant packets within the same sending cycle.
3) When the node with physical ID 20 finishes its sending cycle, one sending round completes. To avoid overlapping of packet transmission, after the node with physical ID 1 receives synchronization packets sent by the node with physical ID 20, ID 1 node will wait one minute and start over another sending round.
4) Repeat the above steps. In our experiments, we have collected 80 sending rounds of data.

B. Illustrations of Data Collection Procedure

Figure 10 illustrates one sending round of a 5-node network example. Observe the leftmost column first. We denote the physical ID of each node from 1 to 5, starting from the bottom one toward the top one, respectively. In the beginning, the node

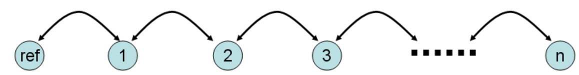

Fig. 11. Topology of the simulated network.

with physical ID 1 broadcasts 10 synchronization packets, with inter-broadcast period of 10 *ms*. Other nodes, which receive any of these packets, record the sending time stamp embedded in the first synchronization packet they receive and disregard others. After the node with physical ID 1 completes broadcasting 10 packets, the node with physical ID 2 waits for 150*ms*, and starts broadcasting 10 synchronization packets as plotted in the second column in Figure 10. The remaining nodes repeat the above process according to their physical ID until every one finishes broadcasting synchronization packets, thus finishing one sending round.

C. Multihop Error Calculation

The scheme of data collection makes it possible to manipulate the data to simulate various combinations of real-world time synchronization. Only a small percentage of data is used in the calculation for each permutation. We used a Matlab program to simulate all three synchronization schemes based on the traces we acquired.

In our simulations, we simulate a network hierarchy of 19 hops with exactly one node in each level as depicted in Figure 11. Therefore, each node can be uniquely identified by its level position in the virtually formed network. The node which provides the reference clock for all other nodes is located in level 0. Synchronization task is taken placed according to the level number.

Since we only have 20 Tmote, in order to simulate the situation of doing synchronization experiments by different devices with the same network topology many times, we shuffle the physical ID and randomly form a 19-hop linear network every time we proceed our error calculation. For example, the level 1 node in the virtual network may be the physical ID 5 node in the first iteration, but becomes the physical ID 15 node in other iteration. Every shuffle operation is independent. In the beginning of each iteration, we first determine the formation of a virtual network. Because a node may receive more than one synchronization packet in each sending cycle, we choose the first one, which is commonly received by all nodes, within each sending cycle to proceed the following computations. All other successful reception within the same sending cycle will be disregarded, and only one packet per sending cycle, per transmitter will be recorded. Based on the way we choose a synchronization packet, in order to guarantee the existence of at least one such packet in each sending cycle, every node broadcast 10 packets, instead of 1, within its sending cycle. Thus, the robustness to possible failure of transmission during data collection procedure is ensured.

In addition, if we want to synchronize the level i and $i+1$ node, which correspond to physical ID l and m, the k-th packet in this synchronization task is the one transmitted between node l and m, from $2(i-1)+k$ sending round. An example can be found in the next section.

The synchronization error contributed by level i is computed by the clock difference between calibrated level i clock reading and the corresponding reference node clock reading at the same instance.

Whenever we finish synchronizing a pair of nodes, we know the relative drift estimation between these two nodes by using formulas stated in Sections III. Therefore, we have choices of using relative drift estimation to calibrate clock readings or not, before a synchronized level i node needs to provide time stamps to the node resided in its immediate descent level, $i+1$. In order to verify the impact of inter-sync error under different scenario, we adopt both strategies in later sections.

We repeat the above process for the remaining nodes, and consider the completion of synchronization tasks of every node in a virtually formed network as one iteration of synchronization simulation. The above procedure is repeated for 100 times, and choice of packets are made independently every time. The propagation error in every level is then calculated by averaging the outcomes of 100 synchronization iterations within the same level.

D. Illustrations of Multihop Error Calculation

Consider a simple scenario as follows. Suppose we only use 6 Tmote, with physical ID from A to F, and have already collected 12 sending rounds of data by following the previously stated procedure. In the beginning, we first randomly shuffle the physical ID and the resulting virtual network is listed in Table IV. One-way synchronization scheme is adopted in this example.

In Figure 12, we plot the packets exchange scheme of our example. The X-axis and the Y-axis represent the ideal time and the level number in our virtually formed network, respectively. The reference node is located in level 1 in this example. Each arrow represent a synchronization packet transmission, while the head and tail of a arrow is attached to the receiver and the sender for that packet, respectively. Take the two packets between level 2 and 3 in Figure 12 for example. The first and second of these two packets is chosen from the $2\times(2-1)+1 = 3$-th and $2\times(2-1)+2 = 4$-th sending round, respectively. Then, do linear regression on the sender and receiver time stamps retrieved from these two packets to calculate the drift and relative drift estimation between E and A. Thereafter, we use the calculated drift and relative drift

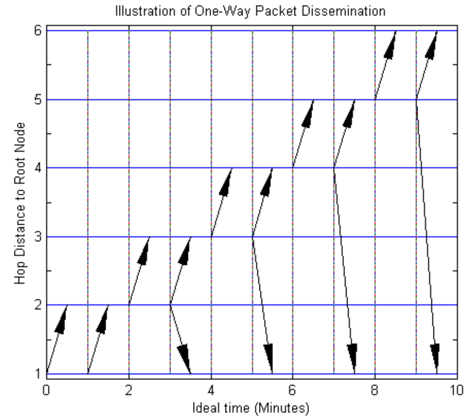

Fig. 12. Example packet exchange scenario for calculating propagation error using one-way scheme.

estimation to predict node A clock reading after calibration under one-way scheme. Since both these two packets are also received by the reference node, which has physical ID C, we use the time the reference node receives these packets as an approximation to the ideal time and find out the multihop propagation error in this level by computing clock difference between the calibrated A reading and the corresponding node C clock reading. We call this error as "2-hop propagation error".

Note that, base on this method, we can thus have several virtually formed 19-hop linear networks by randomly shuffling physical ID in the data we collected from our experiments. The results presented later are calculated by averaging propagation errors acquired from 100 randomly formed networks.

VI. Results and Discussion

A. Predicted outcomes

In the trace based simulations, we have the following conditions which are relevant to our analysis models:

- The time periods between two consecutive packets within the same synchronization task are approximately the same. In other words, T_{intra} is a constant throughout the whole experiments.
- The time period between two consecutive synchronization process, i.e. the duration between the end of a synchronization process and the beginning of the next immediate process, is approximately the same. In other words, T_{inter} is a constant throughout the whole experiments.
- $T_{inter} \approx T_{intra}$.

By applying the above conditions to our analysis, we can predict the outcomes of our experiments as listed in table VI and V. The former adopts relative drift estimation to compensate for inter-sync error under different schemes, whereas the later does not.

B. Experiment Results

The average 19-hop propagation error with relative drift compensation of all three synchronization schemes are listed in table VI and plotted in figure 14. The outcomes presented are

Level number	1	2	3	4	5	6
Physical ID	C	E	A	F	B	D

TABLE IV

AN EXAMPLE OF VIRTUALLY FORMED NETWORK.

	One-Way	Two-Way	Hybrid
Measured Average Overall Propagation Error	167.4 ms	- 0.2 ms	0.38 ms
Predicted Average Overall Propagation Error (Θ^{19})	$19 \times (E[\Gamma])$	≈ 0	≈ 0
Measured Average Per-hop Propagation Error	8.8 ms	- 0.0105 ms	0.02 ms
Predicted Average Per-hop Propagation Error ($\Theta^{19}/19$)	$E[\Gamma]$	≈ 0	≈ 0

TABLE V

PROPAGATION ERROR UNDER DIFFERENT SYNCHRONIZATION SCHEMES WITHOUT INTER-SYNC ERROR COMPENSATION

	One-Way	Two-Way	Hybrid
Measured Average Overall Propagation Error	176 ms	4535 ms	-0.18 ms
Predicted Average Overall Propagation Error (Θ^{19})	$19 \times (E[\Gamma])$	$510 \times (E[\Gamma])$	≈ 0
Measured Average Per-hop Propagation Error	9.26 ms	238.7 ms	-0.0.095 ms
Estimated Average Per-hop Propagation Error ($\Theta^{19}/19$)	$E[\Gamma]$	$26.8 \times (E[\Gamma])$	≈ 0

TABLE VI

PROPAGATION ERROR UNDER DIFFERENT SYNCHRONIZATION SCHEMES WITH INTER-SYNC ERROR COMPENSATION

	variance
Two-way without inter-sync error compensation at 19-hop	220.8
Hybrid with inter-sync error compensation at 19-hop	19.4

TABLE VII

VARIANCE OF PROPAGATION ERROR COMPARISON

averaged over 100 synchronization iterations. For comparison purpose, we list the results side by side to the predicted outcomes. In table V and figure 13, we present the average 19-hop propagation error without relative drift compensation of all three synchronization schemes. Again, the outcomes presented are also averaged over 100 synchronization iterations, and we list the analysis results for reference.

As listed in table VI, the hybrid scheme possesses the lowest error, while two-way scheme performs the highest error. A more interesting conclusion can be made by observing figure 14. One-way scheme maintains a linearly increasing trend with respect to the hop distance to the reference node, and propagation error of two-way scheme raises quadratically. Both schemes suffer from unbounded error. On the other hand, hybrid scheme not only performs significantly better precision comparing to the other two schemes under the same settings, most importantly, our hybrid scheme is capable of providing bounded propagation error.

By comparing the one-way scheme with our predicted value, the average of Γ thus can be computed as $167ms/19 \approx 8.8ms$. Similarly, the average value of Γ calculated from two-way scheme can be computed as $4535ms/510 \approx 8.9ms$, which is very close to what we get from one-way calculation. For the hybrid case, while the predicted value is 0, our experiment outcomes show fluctuated propagation error at different hop distance. The reason of this unmatched results is also caused by the high jitter nature of how we do time stamping. In figure 15 we plot the distribution of Γ we calculated from the traces. While the mean of Γ is around 8.9 ms, the standard deviation is 2.3. In both one-way and two-way scheme, since the mean propagation error is large, the fluctuation caused by the variance is not obvious at all. However, the hybrid scheme is very precise such that little fluctuations will be easily observed. Based on the above discussions, all these experiment outcomes verify our analysis conclusions.

In table V, although one-way and hybrid scheme still performs similarly as they do in previous setting, two-way scheme possesses considerably lower propagation error comparing with the prior settings. Especially, two-way scheme, as hybrid scheme, shows no obvious trend of increasing propagation while hop distance goes up in Figure 13, and the synchronization precision of both two-way and hybrid schemes are comparable. This results also match our prediction. From the one-way side, because of the precise relative drift estimation, most of the inter-sync error can be eliminated efficiently. Thus only the drift estimation error will propagate hop by hop. By calculating the average value of $E[\Gamma]$ from the experiment outcomes, we get $171ms/19 \approx 8.9ms$, which is the same as prior value. For the hybrid scheme, because it is capable of providing accurate drift and relative drift estimations simultaneously, the results presented also match our expectation. For the two-way scheme, due to the precise drift estimation we can get from it, the remaining error sources are the relative drift taken place during inter and intra synchronization period. However, because of the equal probability that the actual clock frequency of one node is faster or slower than the other clock that intends to synchronize with itself, it can be expected that the relative drift terms are equally likely to get

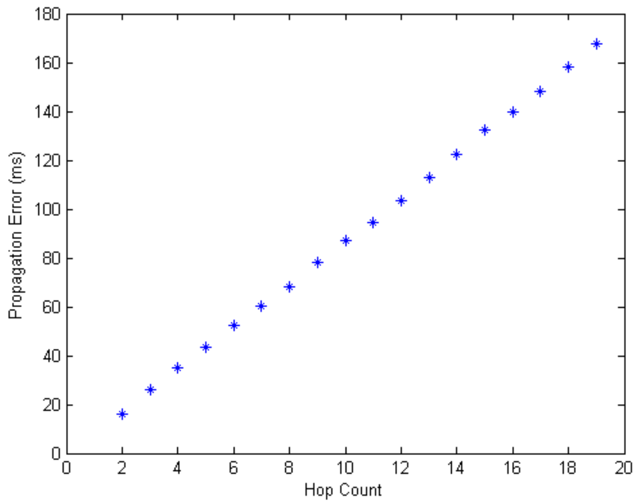

(a) One-way

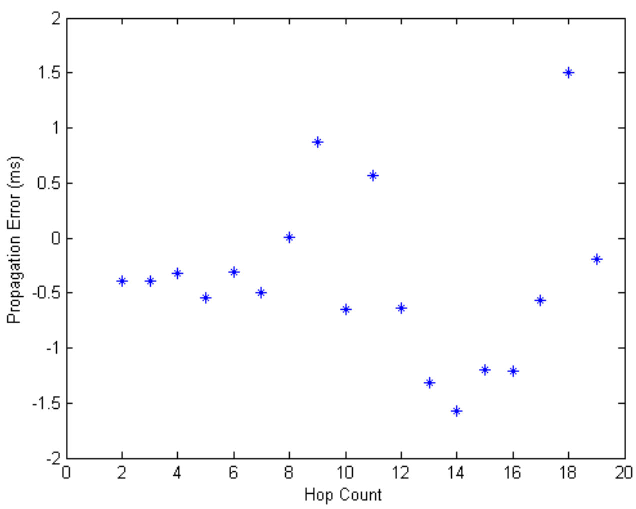

(b) Two-way

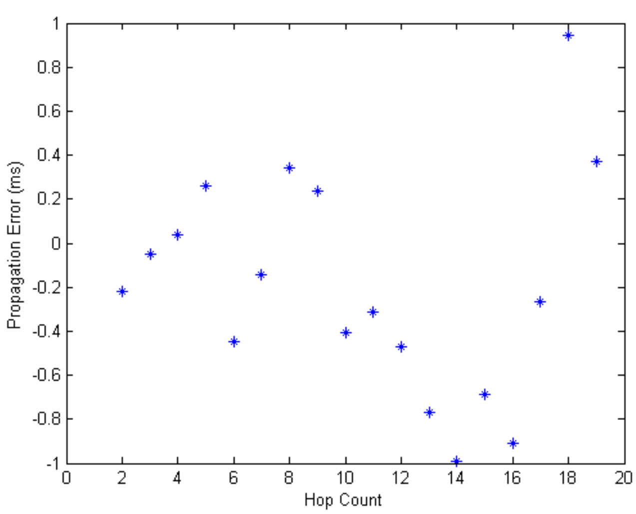

(c) Hybrid

Fig. 13. Trace based simulation results showing multi-hop error propagation for one-way, two-way and hybrid schemes without inter-sync error compensation.

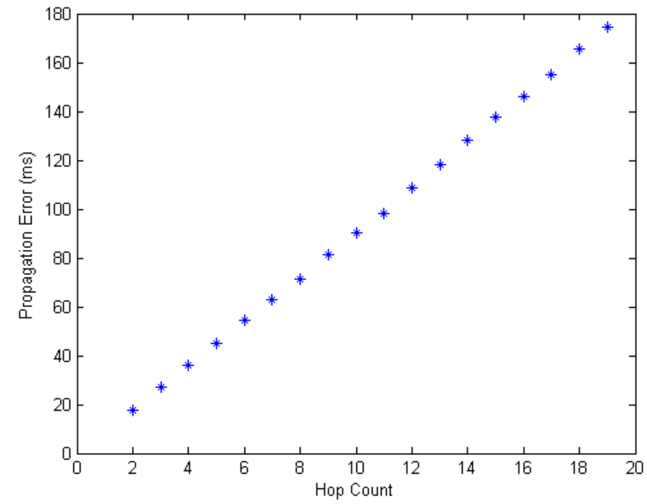

(a) One-way

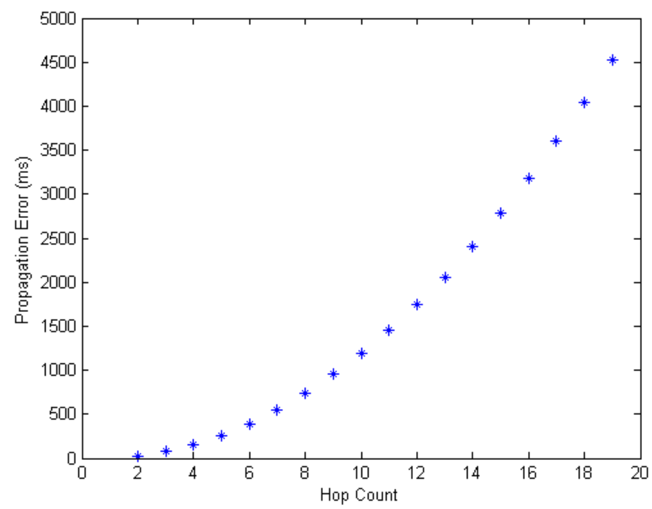

(b) Two-way

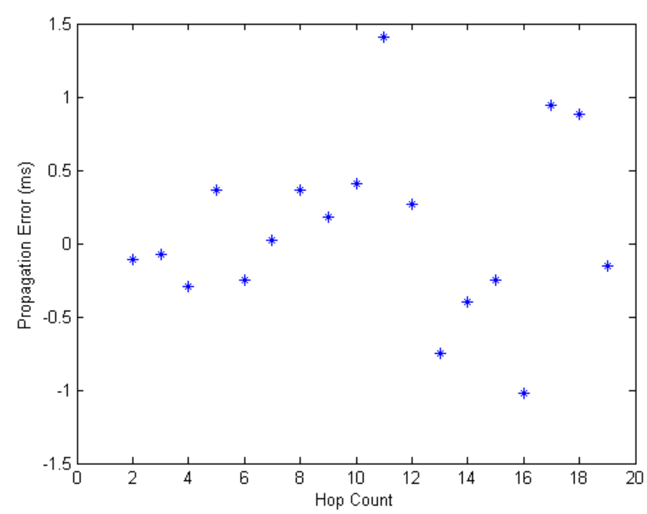

(c) Hybrid

Fig. 14. Trace based simulation results showing multi-hop error propagation for one-way, two-way and hybrid schemes with inter-sync error compensation.

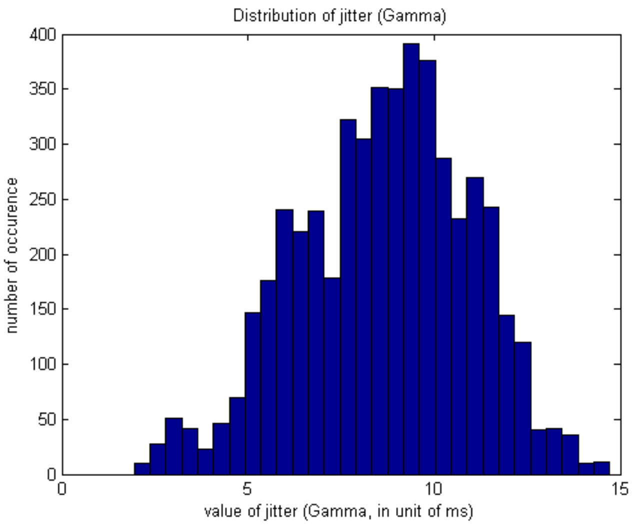

Fig. 15. Distribution of Γ.

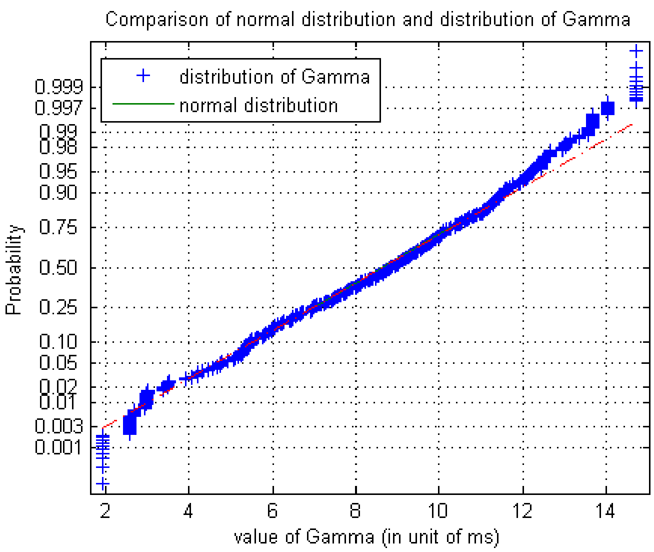

Fig. 16. Distribution of Γ vs. normal distribution.

positive and negative values. In addition, the value of T_{inter} and T_{intra} is a constant in our trace based simulations, it is also reasonable to expect the relative drift will cancel each other throughout different synchronization iterations. A more detailed descriptions can be found in Appendix II.

C. More comparisons between hybrid and two-way scheme

In our data collection process, because of the small value of T_{inter} and T_{intra}, the advantage of compensating inter-sync error, which is the major difference between hybrid and two-way scheme, can not be fully revealed. In order to verify the efficiency of hybrid scheme, we do one more trace based simulation to simulate the situation such that the inter-sync error dominates the overall propagation error.

Consider the following scenario.

- We generate 20 clocks, each with frequency 32000 *Hz* and bias of δppm , to form a 19-hop linear network. δ has a uniform distribution between $\pm 40ppm$. Each level has only one node, thus each node can be uniquely identified by it is level location as before. The reference node is located at level 0.
- We set the T_{intra} and T_{sync} to be 10 minutes, ie 19.2 million ticks, in our subsequent simulations. Because we are able to figure out the probability distribution of the jitter term (Γ) from the traces we acquire, every time we create a time stamp from the above 20 clocks, a random variable generated from the distribution of Γ is added to each clock reading corresponding to different synchronization schemes.
- We do propagation error analysis exactly as before, and continue the above process for 100 times to calculate the average.

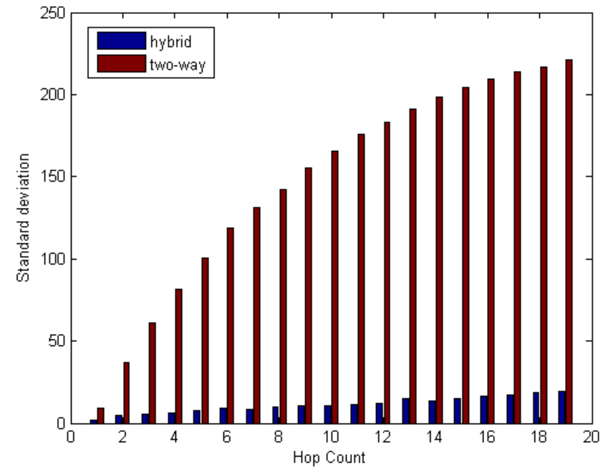

Fig. 17. Comparison between standard deviation of two-way propagation error without inter-sync error compensation and hybrid propagation error with inter-sync error compensation.

Figure 17 is the standard deviation of propagation error of two-way without inter-sync error compensation and hybrid with inter-sync error compensation. In equation (102), the variance of two-way scheme without inter-sync error compensation demonstrates a linearly increasing trend with respect to hop count distance to the reference node. Because standard deviation is the square root of variance, the result plotted in figure (17) matches our prediction. On the other hand, the variance of hybrid scheme with inter-sync error compensation can be computed by equation (101), and is only consisted of variance of Γ terms. Because the variance of Γ terms is significantly smaller than the variance of relative drift terms whenever the value of T_{inter} and T_{intra} are large, it is also reasonable to see lower variance of propagation error of hybrid with inter-sync error compensation comparing with two-way without inter-sync error compensation. The results presented in figure (17) also verify this estimation.

VII. Summary and Future Work

The major contributions of this work are as follows. First, we have presented a thorough comparison of two-way packet exchange, and one-way dissemination schemes, whereby we find that, while one-way dissemination performs worse in estimating drift, two-way dissemination performs worse in estimating relative drift. Second, we have proposed a hybrid one-way dissemination/two-way exchange synchronization scheme that can provide substantially better accuracy, bounded error propagation over multiple hops, and low variance of propagation error. Such a strategy would be most useful for very large scale network deployments. Third, we implement a series of experiment to collect time stamps from real T-motes. From the trace-based simulation results, we get the same conclusions as we make in our analysis.

In the future, we hope to extend this work by doing fine-grained time stamping in practical experiments. In addition, we plan to develop a time synchronization protocol based on the hybrid scheme that will be suitable for multi-hop settings. It would then be of great value to compare the different approaches in detail through real implementations on wireless devices.

VIII. Acknowledgements

Thanks our anonymous reviewers as well as members of the USC Autonomous Networks Research Group for their constructive and valuable feedback on this work.

Appendix I
Effectiveness of Approximation

In order to verify the influence of using the approximation in equation (4) and all similar terms, consider the packet I in figure 3.

Claim: $D_{t1}^{ref \to A} \approx D_{t2}^{ref \to A}$

*Proof:*Due to the fact that imprecision of the clock generater used in T-motes can be as loose as 40*ppm*, in the extreme case, the relative drift generated within 1 second can be as large as:

$$\begin{aligned} \text{relative drift} &= 40ppm \times 2 \times 1second \times 32000Hz \\ &\approx 0.256ticks \end{aligned} \tag{37}$$

According to [2], the typical value of Γ_I is hundreds of ms. Therefore, the approximation of $D_{t1}^{ref \to A} \approx D_{t2}^{ref \to A}$ hardly influences analysis outcomes.

As a immediate result, $RD_{t1 \to t3}^{ref \to A} \approx RD_{t2 \to t4}^{ref \to A}$, $\Gamma_I B_A \approx \Gamma_I$, and so the other similar approximations used in the context.

Appendix II
Influence of relative drift terms

Take equation (11) for example, precision of drift estimation is influenced by one relative drift term, $RD_{t1 \to t4}^{ref \to A}$. It will be of interest to understand the impact caused by relative drift in average.

If we denote the actual clock frequency of a node i by X_j, then the relative drift between node a and b taken place from time $t1$ to $t2$ can be computed as,

$$RD_{t1 \to t2}^{a \to b} = (X_a - X_b) * (t2 - t1)$$

If the value of $(t2 - t1)$ is fixed throughout every synchronization iteration, by the fact that X_i are IID (identically, independently distributed) and $(t2 - t1)$ and X_i are independent, the expected value of the relative drift term in the above equation can be computed as,

$$\begin{aligned} E[RD_{t1 \to t2}^{a \to b}] &= E[(X_a - X_b) * (t2 - t1)] \\ &= E[(X_a - X_b)] * E[(t2 - t1)] = 0 \end{aligned}$$

Thus, the relative drift taken place during $t1$ to $t2$ will not deteriorate the mean of synchronization error. The same conclusion will be hold if similar conditions are satisfied.

Appendix III
Detail derivation of propagation error under different scenarios

A. One-way scheme without inter-sync error compensation

Consider a synchronization scenario as plotted in Figure 7. The drift estimation and actual drift can be calculated as,

$$\beta_{t4}^{i \to i+1} = T4^{ori} - T3^{est} \tag{38}$$

$$D_{t4}^{i \to i+1} = T4^{ori} - T3^{ideal} - \Gamma_{II} \tag{39}$$

Therefore, the propagation error up to $i+1$ hop can be computed as,

$$\begin{aligned} \Theta_{t4}^{i+1} &= T4^{ideal} - T4^{est} \\ &= (T4^{ori} - D_{t4}^{i \to i+1}) - (T4^{ori} - \beta_{t4}^{i \to i+1}) \\ &= -D_{t4}^{i \to i+1} + \beta_{t4}^{i \to i+1} \\ &= T3^{ideal} - T3^{est} + \Gamma_{II} \end{aligned} \tag{40}$$

Similarly,

$$\Theta_{t8}^{i+2} = T7^{ideal} - T7^{est} + \Gamma_{IV} \tag{41}$$

However,

$$T7^{ideal} = T7^{ori} - D_{t4}^{i \to i+1} + RD_{t4 \to t7}^{i \to i+1} \tag{42}$$

$$T7^{est} = T7^{ori} - \beta_{t4}^{i \to i+1} \tag{43}$$

The propagation error up to $i+2$ hop thus becomes,

$$\Theta_{t8}^{i+2} = \Theta_{t4}^{i+1} + RD_{t4 \to t8}^{i \to i+1} + \Gamma_{IV} \tag{44}$$

B. Two-way scheme without inter-sync error compensation

Consider a synchronization scenario as plotted in Figure 8. The drift estimation and its actual value can be computed as,

$$\beta_{t4}^{i \to i+1} = \frac{1}{2}[(T1^{ori} - T2^{est}) - (T3^{est} - T4^{ori})] \tag{45}$$

$$\begin{aligned} D_{t4}^{i \to i+1} &= \frac{1}{2}[(T1^{ori} - T2^{ideal}) - (T3^{ideal} - T4^{ori}) \\ &- RD_{t1 \to t4}^{i \to i+1} + (\Gamma_I - \Gamma_{II})] \end{aligned} \tag{46}$$

Thus, the propagation error up to hop $i+1$ is,

$$\begin{aligned} \Theta_{t4}^{i+1} &= T4^{ideal} - T4^{est} = -D_{t4}^{i \to i+1} + \beta_{t4}^{i \to i+1} \\ &= \frac{1}{2}[(T2^{ideal} - T2^{est}) + (T3^{ideal} - T3^{est}) \\ &+ RD_{t1 \to t4}^{i \to i+1} - (\Gamma_I - \Gamma_{II})] \end{aligned} \tag{47}$$

Again,

$$\beta_{t8}^{i+1\to i+2} = \frac{1}{2}[(T5^{ori} - T6^{est}) - (T7^{est} - T8^{ori})] \quad (48)$$

$$\begin{aligned} D_{t8}^{i+1\to i+2} &= \frac{1}{2}[(T5^{ori} - T2^{ideal}) - (T7^{ideal} - T8^{ori}) \\ &- RD_{t5\to t8}^{i+1\to i+2} + (\Gamma_{III} - \Gamma_{IV})] \end{aligned} \quad (49)$$

$$\begin{aligned} \Theta_{t8}^{i+2} &= T8^{ideal} - T8^{est} \\ &= -D_{t8}^{i+1\to i+2} + \beta_{t8}^{i+1\to i+2} \\ &= \frac{1}{2}[(T6^{ideal} - T6^{est}) + (T7^{ideal} - T7^{est}) \\ &+ RD_{t5\to t8}^{i+1\to i+2} - (\Gamma_{III} - \Gamma_{IV})] \end{aligned} \quad (50)$$

Because $T6^{ideal}$, $T6^{est}$, $T7^{ideal}$, and $T7^{est}$ can be computed as,

$$T6^{ideal} = T6^{ori} - D_{t4}^{i\to i+1} + RD_{t4\to t6}^{i\to i+1} \quad (51)$$

$$T6^{est} = T6^{ori} - \beta_{t4}^{i\to i+1} \quad (52)$$

$$T7^{ideal} = T7^{ori} - D_{t4}^{i\to i+1} + RD_{t4\to t7}^{i\to i+1} \quad (53)$$

$$T7^{est} = T7^{ori} - \beta_{t4}^{i\to i+1} \quad (54)$$

Thus, Θ_{t8}^{i+2} becomes,

$$\begin{aligned} \Theta_{t8}^{i+2} &= \frac{1}{2}[-2(D_{t4}^{i\to i+1} - \beta_{t4}^{i\to i+1}) + RD_{t4\to t6}^{i\to i+1} \\ &+ RD_{t4\to t7}^{i\to i+1} + RD_{t5\to t8}^{i+1\to i+2} - (\Gamma_{III} - \Gamma_{IV})] \\ &= \frac{1}{2}[2\Theta_{t4}^{i+1} + RD_{t4\to t6}^{i\to i+1} + RD_{t4\to t7}^{i\to i+1} \\ &+ RD_{t5\to t8}^{i+1\to i+2} - (\Gamma_{III} - \Gamma_{IV})] \end{aligned} \quad (55)$$

C. Hybrid scheme without inter-sync error compensation

Consider a synchronization scenario as plotted in Figure 9. The drift estimation and its actual value can be computed as,

$$\begin{aligned} \beta_{t6}^{i\to i+1} &\approx \frac{1}{2}[(T6^{ori} - T4^{est}) - (T5^{est} - T3^{ori}) \\ &+ \frac{T_{intra}}{2T_{intra}}[(T6^{ori} - T2^{ori}) - (T5^{est} - T1^{est})]] \end{aligned} \quad (56)$$

$$\begin{aligned} D_{t6}^{i\to i+1} &\approx \frac{1}{2}[(T6^{ori} - T4^{ideal}) - (T5^{ideal} - T3^{ori}) \\ &+ \frac{T_{intra}}{2T_{intra}}[(T6^{ori} - T2^{ori}) - (T5^{ideal} - T1^{ideal}) \\ &- (\Gamma_{III} - \Gamma_{I})] - (\Gamma_{III} - \Gamma_{II})] \end{aligned} \quad (57)$$

Thus, the propagation error up to hop $i+1$ is,

$$\begin{aligned} \Theta_{t6}^{i+1} &= T6^{ideal} - T6^{est} = -D_{t6}^{i\to i+1} + \beta_{t6}^{i\to i+1} \\ &\approx \frac{1}{2}[(T4^{ideal} - T4^{est}) + (T5^{ideal} - T5^{est}) \\ &+ \frac{T_{intra}}{2T_{intra}}[(T5^{ideal} - T5^{est}) \\ &- (T1^{ideal} - T1^{est}) + (\Gamma_{III} - \Gamma_{I})] \\ &+ (\Gamma_{III} - \Gamma_{II})] \end{aligned} \quad (58)$$

Again,

$$\begin{aligned} \beta_{t12}^{i+1\to i+2} &\approx \frac{1}{2}[(T12^{ori} - T10^{est}) - (T11^{est} - T9^{ori}) \\ &+ \frac{T_{intra}}{2T_{intra}}[(T12^{ori} - T8^{ori}) - (T11^{est} - T7^{est})]] \end{aligned} \quad (59)$$

$$\begin{aligned} D_{t12}^{i+1\to i+2} &\approx \frac{1}{2}[(T12^{ori} - T10^{ideal}) - (T11^{ideal} - T9^{ori}) \\ &+ \frac{T_{intra}}{2T_{intra}}[(T12^{ori} - T8^{ori}) - (T11^{ideal} - T7^{ideal}) \\ &- (\Gamma_{VI} - \Gamma_{IV})] - (\Gamma_{VI} - \Gamma_{V})] \end{aligned} \quad (60)$$

Because the calibrated clock readings are,

$$T7^{est} = T7^{ori} - \beta_{t6}^{i\to i+1} \quad (61)$$

$$T7^{ideal} = T7^{ori} - D_{t6}^{i\to i+1} + RD_{t6\to t7}^{i\to i+1} \quad (62)$$

$$T10^{est} = T10^{ori} - \beta_{t6}^{i\to i+1} \quad (63)$$

$$T10^{ideal} = T10^{ori} - D_{t6}^{i\to i+1} + RD_{t6\to t10}^{i\to i+1} \quad (64)$$

$$T11^{est} = T11^{ori} - \beta_{t6}^{i\to i+1} \quad (65)$$

$$T11^{ideal} = T11^{ori} - D_{t6}^{i\to i+1} + RD_{t6\to t11}^{i\to i+1} \quad (66)$$

therefore, propagation error up to $i+2$ hop becomes,

$$\begin{aligned} \Theta_{t12}^{i+2} &= T12^{ideal} - T12^{est} \\ &= -D_{t12}^{i+1\to i+2} + \beta_{t12}^{i+1\to i+2} \\ &\approx \frac{1}{2}[(T10^{ideal} - T10^{est}) + (T11^{ideal} - T11^{est}) \\ &+ \frac{T_{intra}}{2T_{intra}}[(T11^{ideal} - T11^{est}) \\ &- (T7^{ideal} - T7^{est}) + (\Gamma_{VI} - \Gamma_{IV})] + (\Gamma_{VI} - \Gamma_{V})] \\ &\approx \frac{1}{2}[2\Theta_{t6}^{i+1} + (RD_{t6\to t10}^{i\to i+1} + \frac{3}{2}RD_{t6\to t11}^{i\to i+1}) \\ &- \frac{1}{2}RD_{t6\to t7}^{i\to i+1} + (\frac{3}{2}\Gamma_{VI} - \frac{1}{2}\Gamma_{IV} - \Gamma_{V})] \end{aligned} \quad (67)$$

D. One-way scheme with inter-sync error compensation

Consider the scenario plotted in Figure 7. $\beta_{t4}^{i\to i+1}$, $D_{t4}^{i\to i+1}$, and Θ_{t4}^{i+1} are identical to equation (38), (39), and (40). $\alpha_{t2\to t4}^{i\to i+1}$ and $RD_{t2\to t4}^{i\to i+1}$ can be calculated as,

$$\alpha_{t2\to t4}^{i\to i+1} = (T2^{ori} - T4^{ori}) - (T1^{est} - T3^{est}) \quad (68)$$

$$\begin{aligned} RD_{t2\to t4}^{i\to i+1} &= (T2^{ori} - T4^{ori}) \\ &-(T1^{ideal} - T3^{ideal}) - (\Gamma_{I} - \Gamma_{II}) \end{aligned} \quad (69)$$

Therefore, $\Phi_{t2\to t4}^{i\to i+1}$ is,

$$\begin{aligned} \Phi_{t2\to t4}^{i\to i+1} &= RD_{t2\to t4}^{i\to i+1} - \alpha_{t2\to t4}^{i\to i+1} \\ &= (T3^{ideal} - T3^{est}) - (T1^{ideal} - T1^{est}) - (\Gamma_{I} - \Gamma_{II}) \end{aligned} \quad (70)$$

Because $T7^{ideal}$ and $T7^{est}$ is,

$$\begin{aligned} T7^{ideal} &= T7^{ori} - D_{t4}^{i\to i+1} + RD_{t4\to t7}^{i\to i+1} \\ &\approx T7^{ori} - T4^{ori} + T3^{ideal} + \Gamma_{II} \\ &+ \frac{T_{inter} + T_{intra}}{T_{intra}}[(T2^{ori} - T4^{ori}) \\ &- (T1^{ideal} - T3^{ideal}) - (\Gamma_{I} - \Gamma_{II})] \end{aligned} \quad (71)$$

$$
\begin{aligned}
T7^{est} &= T7^{ori} - \beta_{t4}^{i\to i+1} + \alpha_{t4\to t7}^{i\to i+1} \\
&\approx T7^{ori} - T4^{ori} + T3^{est} \\
&+ \frac{T_{inter}+T_{intra}}{T_{intra}}[(T2^{ori} - T4^{ori}) \\
&- (T1^{est} - T3^{est})] \qquad (72)
\end{aligned}
$$

thus, propagation error up to $i+2$ hop can be computed as,

$$
\begin{aligned}
\Theta_{t8}^{i+2} &= T8^{ideal} - T8^{est} \\
&= T7^{ideal} - T7^{est} + \Gamma_{IV} \\
&\approx (T3^{ideal} - T3^{est}) + \Gamma_{II} \\
&+ \frac{T_{inter}+T_{intra}}{T_{intra}}[(T3^{ideal} - T3^{est}) \\
&- (T1^{ideal} - T1^{est}) - (\Gamma_I - \Gamma_{II})] + \Gamma_{IV} \\
&= \Theta_{t4}^{i+1} + \frac{T_{inter}+T_{intra}}{T_{intra}}\Phi_{t2\to t4}^{i\to i+1} + \Gamma_{IV} \qquad (73)
\end{aligned}
$$

In addition,

$$
\begin{aligned}
\Phi_{t6\to t8}^{i+1\to i+2} &= RD_{t6\to t8}^{i+1\to i+2} - \alpha_{t6\to t8}^{i+1\to i+2} \\
&= \Phi_{t2\to t4}^{i\to i+1} - (\Gamma_{III} - \Gamma_{IV}) \qquad (74)
\end{aligned}
$$

E. Two-way scheme with inter-sync error compensation

Refer to an example scenario plotted in Figure 8. $\beta_{t4}^{i\to i+1}$, $D_{t4}^{i\to i+1}$, and Θ_{t4}^{i+1} are identical to equation (45), (46), and (47). $\alpha_{t1\to t4}^{i\to i+1}$, $RD_{t1\to t4}^{i\to i+1}$, and $\Phi_{t1\to t4}^{i\to i+1}$ can be calculated as,

$$
\alpha_{t1\to t4}^{i\to i+1} = (T1^{ori} - T2^{est}) + (T3^{est} - T4^{ori}) \qquad (75)
$$

$$
\begin{aligned}
RD_{t1\to t4}^{i\to i+1} &= (T1^{ori} - T2^{ideal}) \\
&+(T3^{ideal} - T4^{ori}) + (\Gamma_I + \Gamma_{II}) \qquad (76)
\end{aligned}
$$

$$
\begin{aligned}
\Phi_{t1\to t4}^{i\to i+1} &= RD_{t1\to t4}^{i\to i+1} - \alpha_{t1\to t4}^{i\to i+1} \\
&= (T2^{est} - T2^{ideal}) - (T3^{est} - T3^{ideal}) \\
&+ (\Gamma_I + \Gamma_{II}) \qquad (77)
\end{aligned}
$$

Similarly, we can have,

$$
\beta_{t8}^{i+2} = \frac{1}{2}[(T5^{ori} - T6^{est}) - (T7^{est} - T8^{ori})] \qquad (78)
$$

$$
\alpha_{t5\to t8}^{i+1\to i+2} = (T5^{ori} - T6^{est}) + (T7^{est} - T8^{ori}) \qquad (79)
$$

The value of clock readings compensated by relative drift estimation thus becomes,

$$
T6^{est} = T6^{ori} - \beta_{t4}^{i\to i+1} + \alpha_{t1\to t4}^{i\to i+1}\frac{T6^{ori} - T4^{ori}}{T4^{ori} - T1^{ori}} \qquad (80)
$$

$$
T7^{est} = T7^{ori} - \beta_{t4}^{i\to i+1} + \alpha_{t1\to t4}^{i\to i+1}\frac{T7^{ori} - T4^{ori}}{T4^{ori} - T1^{ori}} \qquad (81)
$$

And the error of these calibrated readings,

$$
\begin{aligned}
&T6^{ideal} - T6^{est} \\
&= -D_{t4}^{i\to i+1} + \beta_{t4}^{i\to i+1} + RD_{t4\to t6}^{i\to i+1} - \beta_{t4\to t6}^{i\to i+1} \\
&\approx \Theta_{t4}^{i\to i+1} + \frac{T_{inter}}{T_{intra}}\Phi_{t1\to t4}^{i\to i+1} \qquad (82)
\end{aligned}
$$

$$
\begin{aligned}
&T7^{ideal} - T7^{est} \\
&= -D_{t4}^{i\to i+1} + \beta_{t4}^{i\to i+1} + RD_{t4\to t7}^{i\to i+1} - \beta_{t4\to t7}^{i\to i+1} \\
&\approx \Theta_{t4}^{i\to i+1} + \frac{T_{inter}+T_{intra}}{T_{intra}}\Phi_{t1\to t4}^{i\to i+1} \qquad (83)
\end{aligned}
$$

We can thus calculate Θ_{t8}^{i+2} and $\Phi_{t5\to t8}^{i+1\to i+2}$ as follows,

$$
\begin{aligned}
\Theta_{t8}^{i+2} &= -D_{t8}^{i+1\to i+2} - \beta_{t8}^{i+1\to i+2} \\
&= \frac{1}{2}[(T6^{ideal} - T6^{est}) + (T7^{ideal} - T7^{est}) \\
&+ RD_{t5\to t8}^{i+1\to i+2} - (\Gamma_{III} - \Gamma_{IV})] \\
&\approx \Theta_{t4}^{i+1} - \frac{2T_{inter}+T_{intra}}{2T_{intra}}\Phi_{t1\to t4}^{i\to i+1} \\
&+ \frac{1}{2}RD_{t5\to t8}^{i+1\to i+2} + \frac{1}{2}(\Gamma_{IV} - \Gamma_{III}) \qquad (84)
\end{aligned}
$$

$$
\begin{aligned}
\Phi_{t5\to t8}^{i+1\to i+2} &= RD_{t5\to t8}^{i+1\to i+2} - \alpha_{t5\to t8}^{i+1\to i+2} \\
&= (T7^{ideal} - T7^{est}) - (T6^{ideal} - T6^{est}) \\
&+ (\Gamma_{III} + \Gamma_{IV}) \\
&= \Phi_{t1\to t4}^{i\to i+1} + (\Gamma_{III} + \Gamma_{IV}) \qquad (85)
\end{aligned}
$$

F. Hybrid scheme with inter-sync error compensation

Consider the synchronization scenario as plotted in Figure 9. $\beta_{t6}^{i\to i+1}$, $D_{t6}^{i\to i+1}$, and $\Theta_{t6}^{i\to i+1}$ is identical to equation (56), (57), and (58), respectively.

The drift and relative drift estimations and their ideal values are then,

$$
\begin{aligned}
\beta_{t12}^{i+1\to i+2} &\approx \frac{1}{2}[(T12^{ori} - T10^{est}) - (T11^{est} - T9^{ori}) \\
&+\frac{T_{intra}}{2T_{intra}}[(T12^{ori} - T8^{ori}) - (T11^{est} - T7^{est})]] \qquad (86)
\end{aligned}
$$

$$
\begin{aligned}
D_{t12}^{i+1\to i+2} &\approx \frac{1}{2}[(T12^{ori} - T10^{ideal}) - (T11^{ideal} - T9^{ori}) \\
&+ \frac{T_{intra}}{2T_{intra}}[(T12^{ori} - T8^{ori}) - (T11^{ideal} - T7^{ideal}) \\
&- (\Gamma_{VI} - \Gamma_{IV})] - (\Gamma_{VI} - \Gamma_V)] \qquad (87)
\end{aligned}
$$

$$
\alpha_{t3\to t6}^{i\to i+1} \approx \frac{T_{intra}}{2T_{intra}}[(T5^{est} - T1^{est}) - (T6^{ori} - T2^{ori})] \qquad (88)
$$

$$
\begin{aligned}
RD_{t3\to t6}^{i\to i+1} &\approx \frac{T_{intra}}{2T_{intra}}[(T5^{ideal} - T1^{ideal}) \\
&- (T6^{ori} - T2^{ori}) + (\Gamma_{III} - \Gamma_I)] \qquad (89)
\end{aligned}
$$

Therefore,

$$
\begin{aligned}
\Phi_{t3\to t6}^{i\to i+1} &= RD_{t3\to t6}^{i\to i+1} - \alpha_{t3\to t6}^{i\to i+1} \\
&= \frac{T_{intra}}{2T_{intra}}[(T5^{ideal} - T5^{est}) \\
&- (T1^{ideal} - T1^{est}) + (\Gamma_{III} - \Gamma_I)] \qquad (90)
\end{aligned}
$$

In addition, the calibrated clock readings can be computed as,

$$
T7^{est} \approx T7^{ori} - \beta_{t6}^{i\to i+1} + \alpha_{t3\to t6}^{i\to i+1}\frac{T_{inter}}{T_{intra}} \qquad (91)
$$

$$
T7^{ideal} \approx T7^{ori} - D_{t6}^{i\to i+1} + RD_{t3\to t6}^{i\to i+1}\frac{T_{inter}}{T_{intra}} \qquad (92)
$$

$$T10^{est} \approx T7^{ori} - \beta_{t6}^{i\to i+1} + \alpha_{t3\to t6}^{i\to i+1}\frac{T_{inter}+T_{intra}}{T_{intra}} \quad (93)$$

$$T10^{ideal} \approx T10^{ori} - D_{t6}^{i\to i+1} + RD_{t3\to t6}^{i\to i+1}\frac{T_{inter}+T_{intra}}{T_{intra}} \quad (94)$$

$$T11^{est} \approx T11^{ori} - \beta_{t6}^{i\to i+1} + \alpha_{t3\to t6}^{i\to i+1}\frac{T_{inter}+2T_{intra}}{T_{intra}} \quad (95)$$

$$T11^{ideal} \approx T11^{ori} - D_{t6}^{i\to i+1} + RD_{t3\to t6}^{i\to i+1}\frac{T_{inter}+2T_{intra}}{T_{intra}} \quad (96)$$

Therefore, the propagation error up to $i+2$ hop becomes,

$$\begin{aligned}
\Theta_{t12}^{i+2} &= -D_{t12}^{i+1\to i+2} + \beta_{t12}^{i+1\to i+2} \\
&= \frac{1}{2}[(T10^{ideal} - T10^{est}) \\
&+ (T11^{ideal} - T11^{est})(1 + \frac{T12^{ori} - T9^{ori}}{T12^{ori} - T8^{ori}}) \\
&- (T7^{ideal} - T7^{est})\frac{T12^{ori} - T9^{ori}}{T12^{ori} - T8^{ori}} \\
&+ (\frac{T12^{ori} - T9^{ori}}{T12^{ori} - T8^{ori}}(\Gamma_{VI} - \Gamma_{IV}) + \Gamma_{VI} - \Gamma_{V})] \\
&\approx \frac{1}{2}[2\Theta_{t6}^{i+1} + 3\Phi_{t3\to t6}^{i\to i+1} \\
&+ (\frac{T_{intra}}{2T_{intra}}(\Gamma_{VI} - \Gamma_{IV}) + \Gamma_{VI} - \Gamma_{V})] \qquad (97)
\end{aligned}$$

$\alpha_{t9\to t12}^{i+1\to i+2}$, $RD_{t9\to t12}^{i+1\to i+2}$, and $\Phi_{t9\to t12}^{i+1\to i+2}$ can also be calculated as,

$$\begin{aligned}
\alpha_{t9\to t12}^{i+1\to i+2} &\approx \frac{T_{intra}}{2T_{intra}}[(T11^{est} - T6^{est}) \\
&- (T12^{ori} - T8^{ori})] \qquad (98)
\end{aligned}$$

$$\begin{aligned}
RD_{t9\to t12}^{i+1\to i+2} &\approx \frac{T_{intra}}{2T_{intra}}[(T11^{ideal} - T6^{ideal}) \\
&- (T12^{ori} - T8^{ori}) + (\Gamma_{VI} - \Gamma_{IV})] \qquad (99)
\end{aligned}$$

$$\begin{aligned}
\Phi_{t9\to t12}^{i+1\to i+2} &= RD_{t9\to t12}^{i+1\to i+2} - \alpha_{t9\to t12}^{i+1\to i+2} \\
&= \frac{T_{intra}}{2T_{intra}}[(T11^{ideal} - T11^{est}) \\
&- (T7^{ideal} - T7^{est}) + (\Gamma_{VI} - \Gamma_{IV})] \\
&= \frac{1}{2}[(\Gamma_{VI} - \Gamma_{IV}) + 2\Theta_{t3\to t6}^{i\to i+1}] \qquad (100)
\end{aligned}$$

Appendix IV
Variance analysis of two-way and hybrid scheme without inter-sync error compensation

Assume the reference node is located in level i in both schemes.

Consider hybrid with inter-sync error compensation scheme first. In equation (58) and (90), because the only random variables are Γ_I, Γ_{II} and Γ_{III}, the variance of Θ_{t6}^{i+1} and $\Phi_{t3\to t6}^{i\to i+1}$ is,

$$\begin{aligned}
VAR[\Theta_{t6}^{i+1}] &\approx [(\frac{1}{4})^2 + (\frac{1}{4})^2 + (\frac{1}{2})^2 + (\frac{1}{2})^2]VAR[\Gamma] \\
&= \frac{5}{8}VAR[\Gamma]
\end{aligned}$$

$$\begin{aligned}
VAR[\Phi_{t3\to t6}^{i\to i+1}] &\approx [(\frac{1}{2})^2 + (\frac{1}{2})^2]VAR[\Gamma] \\
&= \frac{1}{2}VAR[\Gamma]
\end{aligned}$$

Thus, the variance of propagation error in $i+2$-hop can be computed from (97),

$$\begin{aligned}
&VAR[\Theta_{t12}^{i+2}] \approx VAR[\Theta_{t6}^{i+1}] + (\frac{3}{2})^2 VAR[\Phi_{t3\to t6}^{i\to i+1}] \\
&+ [(\frac{1}{4})^2 + (\frac{1}{2})^2 + (\frac{1}{2})^2 + (\frac{1}{2})^2]VAR[\Gamma] \\
&= VAR[\Theta_{t6}^{i+1}] + \frac{9}{4}VAR[\Phi_{t3\to t6}^{i\to i+1}] + \frac{13}{16}VAR[\Gamma] \\
&= VAR[\Theta_{t6}^{i+1}] + \frac{31}{16}VAR[\Gamma] \qquad (101)
\end{aligned}$$

Because X_i are IID. The variance of Θ_{t4}^{i+1} for two-way without inter-sync error compensation (equation (47)) is,

$$\begin{aligned}
&VAR[\Theta_{t4}^{i+1}] \\
&= (\frac{1}{2})^2 VAR[RD_{t1\to t4}^{i\to i+1}] + [(\frac{1}{2})^2 + (\frac{1}{2})^2]VAR[\Gamma] \\
&= \frac{1}{4}VAR[(X_i - X_{i+1})T_{intra}] + \frac{1}{2}VAR[\Gamma] \\
&= \frac{1}{2}VAR[\Gamma] + \frac{T_{intra}^2}{2}VAR[X]
\end{aligned}$$

Therefore, the variance of Θ_{t8}^{i+2} (equation (55)) becomes,

$$\begin{aligned}
&VAR[\Theta_{t8}^{i+2}] = VAR[\Theta_{t4}^{i+1}] + (\frac{1}{2})^2(VAR[RD_{t4\to t6}^{i\to i+1}] \\
&+ VAR[RD_{t4\to t7}^{i\to i+1}] + VAR[RD_{t5\to t8}^{i+1\to i+2}]) \\
&+ [(\frac{1}{2})^2 + (\frac{1}{2})^2]VAR[\Gamma] \\
&\approx VAR[\Theta_{t4}^{i+1}] + \frac{1}{4}((T_{inter})^2 + (T_{inter})^2)VAR[X] \\
&+ \frac{1}{4}((T_{inter} + T_{intra})^2 + (T_{inter} + T_{intra})^2)VAR[X] \\
&+ \frac{1}{4}((T_{intra})^2 + (T_{intra})^2)VAR[X] + \frac{1}{2}VAR[\Gamma] \\
&= VAR[\Theta_{t4}^{i+1}] + \frac{1}{2}VAR[\Gamma] \\
&+ VAR[X](T_{intra}^2 + T_{inter}^2 + T_{inter}T_{intra}) \qquad (102)
\end{aligned}$$

Propagation error of two-way without inter-sync error compensation always carries high variance to next hop whenever T_{intra} and T_{inter} are large. The situation becomes worse when either of T_{intra} and T_{inter} increases. On the other hand, hybrid scheme with inter-sync error compensation always carries a fixed amount of variance to next hop. Therefore, we can expect to see huge propagation error by using two-way without inter-sync error more frequently than using hybrid scheme with inter-sync error compensation.

References

[1] B. Sundararaman, U. Buy, A.D. Kshemkalyani, "Clock Synchronization in Wireless Sensor Networks: A Survey", *Ad Hoc Networks*, 3(3): 281-323, May 2005.

[2] M. Maroti, B. Kusy, G. Simon and A. Ledeczi, "The Flooding Time Synchronization Protocol," *SenSys*, November 3-5, 2004, Baltimore, Maryland, USA.

[3] S. Ganeriwal, R. Kumar, and M.B. Srivastava, "Timing-sync Protocol for Sensor Networks," *SenSys*, November 5-7, 2003, Los Angeles, California, USA.

[4] J. Elson, L. Girod, and D. Estrin, “Fine-Grained Network Time Synchronization using Reference Broadcasts,” in Proceedings of the Fifth Symposium on Operating Systems Design and Implementation (OSDI 2002), Boston, MA, December 2002.

[5] P. Huang and B. Krishnamachari, “Analysis of existing approaches and a new hybrid strategy for synchronization in sensor networks,” in Proceedings of the Fifth (EmNets 2006), Boston, MA, May 2006.

[6] S. Ganeriwal, D. Ganesan, M. Hansen, M. B. Srivastava, D. Estrin, “Rate-adaptive time synchronization for long-lived sensor networks,” Proceedings of ACM SIGMETRICS international conference on measurement and modeling in computer, June 2005.

[7] B. Krishnamachari, “Networking wireless sensors,” Cambridge university press, 2005.

[8] F. Zhao, L. Guibas, “Wireless sensor networks: an information processing approach,” Morgan Kauffman publisher, 2004.

[9] C. S. Raghavendra, K. M. Sivalingam, T. Znati, “Wireless sensor networks,” kluwer academic publisher, 2004.

[10] R. Karp, J. Elson, D. Estrin, S. Shenker, “Optimal and Global Time Synchronization in Sensornets,” UCLA CENS Technical Report 0012, April 10, 2003.

[11] J. Elson, K. Romer, “Wireless Sensor Networks: A New Regime for Time Synchronization,” Proceedings of the First Workshop on Hot Topics In Networks (HotNets-I), Princeton, New Jersey. October 2002.

[12] F. Sivrikaya, B. Yener, “Time synchronization in sensor networks: a survey,” IEEE Network, July-Aug. 2004, Vol. 18, Issue 4, page 45- 50.

[13] F. Zhang, G. Deng, “Probabilistic time synchronization in wireless sensor networks,” Proceedings of IEEE Wireless Communications, Networking and Mobile Computing, 2005.

Pai-Han Huang obtained his B.E. in Civil Engineering from National Taiwan University in 1998, and his M.S. in Electrical Engineering from University of Southern California in 2005. He is currently an Ph.D. student in the Department of Electrical Engineering-Systems at the University of Southern California. His ongoing research is focused on developing mathematical models for fine grained time synchronization protocols used in sensor networks, delay optimized strategy for multi-hop ad hoc networks, and performance analysis of wireless networks considering receiver diversity schemes.

Maulik Desai obtained B.E. with Honors from The Cooper Union for the Advancement of Science and Art in 2007. At The Cooper Union he was awarded a full tuition scholarship for all four years. In the past he has participated in a team developing a digital receiver front-end for the MRI systems. His current research interest includes employing stochastic modeling techniques to enhance the performance of wireless networks. Maulik Desai is a student member of IEEE, and he is also a member of Eta Kappa Nu, the honor society for the Electrical Engineers.

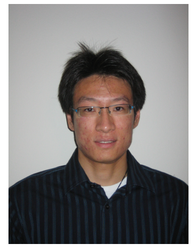

Xiaofan Qiu attended Tsinghua University, Beijing, in 2003. After he finished sophomore year studying Electrical Engineering, he transferred to Texas A&M University, College Station, in 2005. Xiaofan Qiu is completing his senior year of undergraduate study, specializing in analogy circuit design. He is an Undergraduate Research Scholar at Texas A&M. His scholar thesis is “Analysis and characterization of a programmable low-dropout regulator”. He participated in a summer research at University of Southern California, in 2006, studying time synchronization protocols on wireless system. He is also an part-time intern at Hewlett-Packard company.

Bhaskar Krishnamachari obtained his B.E. in Electrical Engineering from The Cooper Union for the Advancement of Science and Art with a four year scholarship in 1998, and his M.S. and Ph.D. in Electrical Engineering from Cornell University in 1999 and 2002 respectively with a full graduate fellowship. Dr. Krishnamachari is currently an Assistant Professor in the Department of Electrical Engineering-Systems at the University of Southern California, with a joint appointment in Computer Science. His ongoing research is focused on developing mathematical models and algorithms for self-configuration and data acquisition/delivery in distributed wireless networks. He is a member of the IEEE and ACM and the Tau Beta Pi and Eta Kappa Nu honor societies.